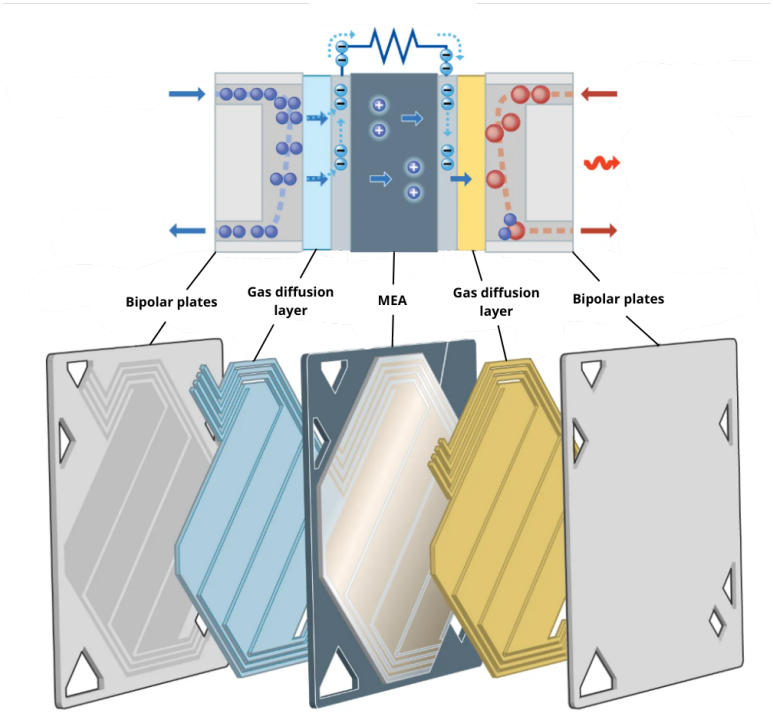

Life Cycle Assessment of Bipolar Plates in Fuel Cell Electric Vehicle Applications

Master's thesis in Sustainable Energy Systems

ANEL HALILOVIC
AGUS ADI PUTRA

DEPARTMENT OF TECHNOLOGY MANAGEMENT AND ECONOMICS
DIVISION OF ENVIRONMENTAL SYSTEMS ANALYSIS

CHALMERS UNIVERSITY OF TECHNOLOGY
Gothenburg, Sweden 2025
www.chalmers.se

REPORT NO.

Life Cycle Assessment of Bipolar Plates in Fuel Cell Electric Vehicle Applications

Anel Halilovic
Agus Adi Putra

Department of Technology Management and Economics
Division of Environmental Systems Analysis
CHALMERS UNIVERSITY OF TECHNOLOGY
Gothenburg, Sweden 2025

Anel Halilovic
Agus Adi Putra

Volvo Group supervisor: Monica Johansson, Fuel and Energy analyst
Hydrogen Infrastructure at Volvo Group

Chalmers supervisor: Natalia Sieti, Department of Technology Management and Economics
Division of Environmental Systems Analysis

Examiner: Mathias Janssen, Department of Technology Management and Economics
Division of Environmental Systems Analysis

Report no. ....
Department of Technology Manegement and Economics
Chalmers University of Technology
SE-412 96 Gothenburg
Sweden
Telephone + 46 (0)31-772 1000

Cover:
Illustration of the components of a proton exchange membrane fuel cell.

Life Cycle Assessment of Bipolar Plates in Fuel Cell Electric Vehicle Applications
An assessment of the environmental impacts and physical properties of three materials for bipolar plates: State-of-the-art composite, Bio-based composite and Metallic

ANEL HALILOVIC
AGUS ADI PUTRA

Department of Technology Manegement and Economics
Chalmers University of Technology

Abstract

This thesis investigates the environmental impact of two types of bipolar plate (BPP) materials used in fuel cell electric vehicles (FCEVs): composite and metallic based BPPs. In total, one steel and four composite BPPs were compared, two biobased and two state-of the-art BPPs.

Using the Life Cycle Assessment (LCA) methodology in accordance with ISO 14040/44 standards, the study evaluates cradle-to-gate impacts across several categories including global warming potential, human toxicity, acidification, and abiotic resource depletion. The data used to model the production of the composites, was from both primary and secondary sources. The metallic BPP data was gathered from secondary sources such as Ecoinvent and literature. OpenLCA was used to model the systems, with a functional unit of 1 kW power output for comparability. This work was carried out in collaboration with the public project BioBPP 2, focused on developing renewable bipolar plates for sustainable fuel cell technology. Results show that the bio-based BPP offers significant potential for environmental impact reduction compared to the other materials. Furthermore, a future scenario with local graphite mining would provide even grater environmental impact reductions. These findings aim to provide valuable insights for stakeholders and support future material development for sustainable fuel cell systems.

Keywords: Life cycle assessment, environmental impacts, fuel cell, bipolar plates

Acknowledgments

We would like to express our sincere gratitude to our supervisor at Chalmers, Natalia Sieti, for her continuous support, valuable feedback, and encouragement throughout this thesis. We are also thankful to our examiner, Mathias Janssen, for his insightful comments and guidance.

A special thanks goes to our industrial supervisor at Volvo Technology, Monica Johansson, for her direction and input for facilitating access to resources that made this work possible. We also wish to thank our colleagues at Volvo for their collaboration and helpful discussions during the project.

We would especially like to thank Guan Gong, from RISE, as a project leader of BioBPP 2, for her support and guidance throughout the course of this work.

We gratefully acknowledge the support of the Ministry of Finance of the Republic of Indonesia, through the Indonesia Endowment Fund for Education (LPDP), for funding Agus Adi Putra's participation in this project and facilitating international collaboration.

Last but not least, we extend our heartfelt gratitude to our families and relatives for their incredible support, which greatly facilitated the completion of this work.

Abbreviations

HDV - *Heavy Duty Vehicle*
BEHDV - *Battery Electric Heavy Duty Vehicle*
HVO - *Hydrogenated Vegetable Oil*
SotA - *State of The Art*
FC - *Fuel Cell*
FCEV - *Fuel Cell Electric Vehicle*
PEM - *Proton Exchange Membrane*
PEMFC - *Proton Exchange Membrane Fuel Cell*
GDL - *Gas Diffusion Layer*
CL - *Catalyst Layer*
BPP - *Bipolar Plates*
BBPP - *Bio-based Bipolar Plates*

LCA - *Life Cycle Assessment*
LCI - *Life Cycle Inventory*
LCIA - *Impact Assessment*
IPCC - *The Intergovernmental Panel on Climate Change*
GWP - *Global Warming Potential*
GHG - *Greenhouse Gas*
PM - *Particulate Matter*
POCP - *Photochemical Ozone Creation Potential*
ILCD - *International Life Cycle Data System*
RISE - *Research Institutes of Sweden*

Contents

List of Figures

List of Tables

1 Introduction

As of 2023, the transport sector accounted for 23% of the world's energy related CO_2 emissions [1]. In 2019, heavy-duty vehicles (HDVs) contributed to 23% of all emissions related to the transport sector [1]. As personal vehicles become more sustainable, HDVs will soon stand out as the major contributors of CO2-emissions and global warming. This, coupled with the importance of honouring the Paris agreement of zero net emissions by 2050, has created a high demand for more sustainable HDVs. Currently, several alternatives are available for HDVs which are far more sustainable than conventional fossil-fuelled vehicles. These options range from conventional combustion vehicles using more sustainable fuels such as hydrogenated vegetable oil (HVO), to battery electric heavy duty vehicles (BEHDVs). Though better for the environment, these options are not always sustainable on the scale needed for them to be suitable options. For example, renewable fuels are in many cases not as sustainable as they may seem due to allocated emissions. While on the other hand insufficient infrastructure and driving range leads BEHDVs to be considered unreliable by many [2].

The technology which has recently been growing in the market for the last couple of years, is the usage of hydrogen as fuel in fuel cell electric vehicles (FCEVs) [3]. The principle behind the FC is as follows: Hydrogen gas gets reduced, leading to a separation of electrons and protons. The electrons move through a circuit. The protons move through a permeable membrane and react with oxygen, resulting in the creation of water, the only by-product of the FCEV. Even though the Hydrogen fuel cell heavy-duty vehicles are promising for the future of HDVs, they currently still contain components with substantial carbon footprints, with the fuel cell being the most significant contributor [4]. Among fuel cell components, bipolar plates significantly influence the overall carbon footprint. Thus, developing innovative materials or manufacturing techniques could lead to a reduction in their environmental impact.

1.1 Motivation for the study

This study is performed in cooperation with RISE on their public project called BioBPP 2. The aim of BioBBP 2 is to design and build one of the first FC short stacks in Sweden [5]. The aim of this study is to aid this project by highlighting the environmental benefits of moving from fossil materials to renewable ones for bipolar plates. Currently, the state-of-the-art bipolar plates are either metallic or composite based, with the most prevalent composite being a mixture of 20 % phenolic resin and 80 % graphite, which will be reffered to as *"SotA composite"* in this report. However, the novel composites which are currently being tested will be called *"SotA composite + biocarbon"* and *"biobased BPP"*. The natural progression is to incorporate more renewable components into the mixture. Hence the next step is to incorporate the both the bio carbon and the bio resin in addition to graphite to increase the renewable content of the bio BPPs, called *"bioBPP + biocarbon"*. All material compositions are presented in Table 1 below.

Table 1: Weight fractions of each component for all bipolar plates.

Bipolar plate	Component	Weight fraction (%)
Bio	Bio-resin	20
	Graphite	80
Bio + biocarbon	Bio-resin	20
	Graphite	70
	Bio-carbon	10
SotA	Phenolic resin	20
	Graphite	80
SotA + biocarbon	Phenolic resin	20
	Graphite	70
	Bio-carbon	10
Metallic	Steel 316	100

This study will put extra focus on bio + biocarbon BPP, as it is expected to have the lowest environmental impact. In total, four different composites and one metallic BPP will also be evaluated to provide a comprehensive comparison of the environmental impacts of the different materials. Furthermore, the thesis will explore an alternative scenario in which material sourcing is conducted locally.

1.2 Research Questions

To achieve the objectives of the projects, the following research questions are expected to be answered.

Q1: How large is the environmental impact generated by bio-based bipolar plates used as the part of fuel cell stack, and in which part of life cycle stage does it have the most dominant impact?

Q2: How does the environmental performance of bio-based bipolar plates compare to that of state-of-art composite and metallic bipolar plates?

Q3: What are the potential trade-offs between environmental impact and performance efficiency for all BPP materials studied?

Q4: In what ways do future scenario on the new material source change the environmental footprint of bio-based bipolar plates?

1.3 Limitations

Throughout the work, multiple limitations have been identified, with the most prominent being the lack of primary data from the suppliers that are a part of the Bio-BPP 2 project, with which we are cooperating. Because of this, many assumptions have needed to be made, based on similar processes from literature or databases. The time frame of the project is also a limitation, as by extending the project timeline, additional primary data could have been obtained. Another limitation, which only becomes apparent after extensive research, is that this industry is highly restrictive in terms of sharing findings. This restrictiveness has resulted in a general lack of accessible secondary data, such as published literature and case studies, which further complicates efforts to validate assumptions and compare results.

2 Technical background of fuel cells

2.1 General structure of a FC

There are several types of fuel cells in both research and market today with the most commonly used being the *proton-exchange membrane fuel cell* (PEMFC). Currently, Volvo trucks are researching and implementing PEMFCs for their *fuel cell electric heavy-duty vehicles* (FCEHDVs). In general, the PEMFC consists of four components, proton exchange membrane, gas diffusion layer (GDL), catalyst layer (CL) and bipolar plates, as illustrated in Figure 1, where *"flow field plate"* is another term for bipolar plate. The PEM is located in the middle of the cell, in between catalyst layers, followed by gas diffusion layers [3]. The most outer component in the FC are the bipolar plates which not only hold the fuel cell together but also allow for the flow of gases and electrons, conducting the electrical current generated from the fuel cell [6]. Each fuel cell only generates a small voltage, typically between 0.5 and 0.7 volts. Therefore to reach the required voltage for the FC system, fuel cell stacks can contain houndreds of bipolar plates which are connected in series [7]. One FC stack currently on the market is the *P-stack* from powercell which uses *stainless steel* (SS) for their BPPs. The number of cells in the P-stack ranges from 275 to 455, based on the rated power output [8]. In addition to the number of cells, the weight and power density of the FC stack in relation to the rated power is presented in Table 2.

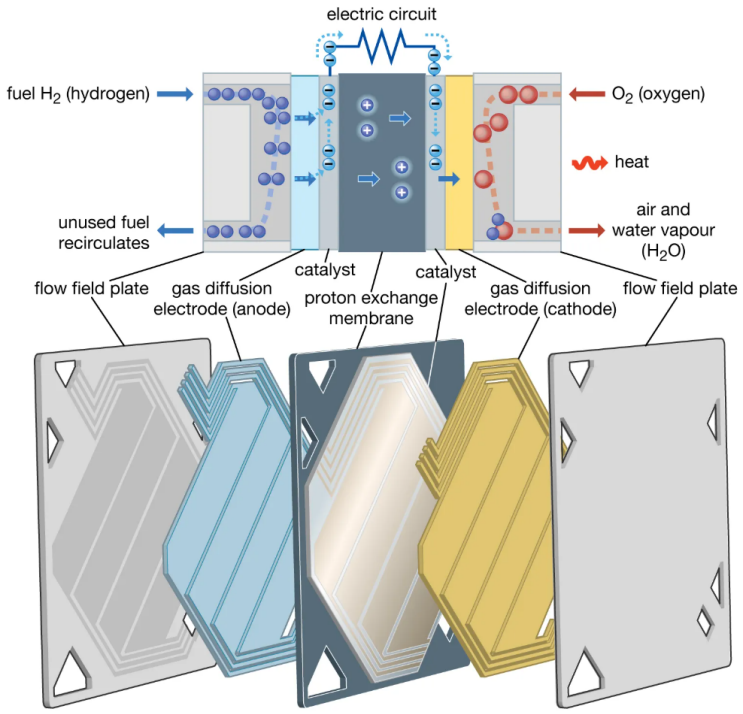

Figure 1: Schematics of a PEMFC [9]

Rated power output	**78 kW**	**95 kW**	**119 kW**	**129 kW**
Fuel cell count	275	335	419	455

Table 2: FC count for each P-stack configuration. [8]

2.2 Working principle

The working principle of the FC is shown in Figure 1, where hydrogen gas (H_2) enters the cell through the bipolar plate on the anode side. Then the hydrogen passes through a gas diffusion layer to spread the gas flow evenly. The hydrogen then passes through the catalyst layer, where the hydrogen gas gets oxidized, splitting the (H_2) molecule into two protons (2 H^+) and two electrons (2 e^-). Due to the nature of the PEM, only protons can pass through it, while the electrons have to pass through an exterior circuit. Simultaneously on the cathode side, oxygen gas (O_2) enters through the bipolar plate and spreads evenly in the cathode GDL. Oxygen passes through the cathode catalyst layer, where the oxygen (O_2) reacts with the incoming protons (H^+) and electrons (e^-), creating water (H_2O), the byproduct of the fuel cell. The transportation of electrons through the exterior circuit makes up the current, which is then used to power electric motors to propel the vehicle [3].

2.3 Proton exchange membrane

As previously implied, the primary function of the PEM is to serve as an electrolyte, enabling the transport of protons from the anode to the cathode. It is crucial that the PEM does not allow the passage of gases such as oxygen or hydrogen. In addition to blocking these gases, electrons are also not able to pass through this membrane, forcing them to travel through an external circuit. The most common material used with these properties is a flexible polymer called Nafion (sulfonated tetrafluoroethylene-based fluoropolymer) [3, 6].

2.4 Catalyst layer

There are two catalyst layers in the fuel cell, one located at the anode and the other at the cathode. Both catalyst layers typically use the same material, with platinum (Pt) being the most common choice due to its excellent catalytic properties. At the anode, the catalyst layer facilitates the splitting of hydrogen molecules (H_2) into two protons (2 H^+) and two electrons (2 e^-). In contrast, the catalyst layer at the cathode has a different function, it facilitates the reduction of oxygen (O_2) by reacting it with the incoming protons and electrons to form water (H_2O) [3].

2.5 Gas diffusion layer

The FC also has two gas diffusion layers which are porous layers with the primary function of spreading the gases evenly. In addition to this, the GDLs are also electron conducting and aid the transportation of electrons between the catalyst layers and the bipolar plates. The GDL also manages the water produced at the cathode by ensuring its removal while retaining enough moisture to keep the PEM hydrated. Lastly, the GDL provides structural integrity to the PEM and CL while ensuring contact between the components under pressure. The most common materials used for the GDL are carbon-based, such as carbon paper or carbon cloth. The carbon paper is a stiff and thin sheet made from carbon fibers, while carbon cloth is a flexible fabric. Usually these materials are coated in *poly tetrafluoroethylene* (PTFE), a hydrophobic substance which improves durability and water management within the FC [3].

2.6 Bipolar plates

Two bipolar plates encapsulate the previously mentioned components, forming the complete fuel cell. The BPPs have multiple crucial roles, with the primary ones being conducting electricity, guiding the gas flows and increasing the structural integrity of the FC [10]. The electron-conductive nature of the BPPs allows for electrons to easily move through the plate [3]. When the FCs are connected in series, electrons move from the BPP to an external circuit and then to the next cell. The BPPs are also responsible for accurately and evenly distributing the flow of hydrogen and oxygen gas into the cell. Therefore, extreme precision is needed during manufacturing in order to prevent inefficient

flow distribution or leakages. Currently, the two most commonly used materials for bipolar plates are composites and metals, which are explained in more detail in the following sections. Additionally, the expected operational lifespan of bipolar plates typically ranges from 5000 to 10000 hours of fuel cell operation [11]. This range serves as a reference for defining the temporal boundaries in LCA studies related to fuel cell components.

2.6.1 Composite bipolar plates

Composite materials consist of two main components: matrix and fillers. For composite BPPs, the matrix is typically a thermoplastic or thermoset polymer such as for example epoxy resin. The main function of the matrix is to act as a binder, holding the composite together by providing mechanical stability. While the matrix covers structural requirements, it deos not conduct electricity well, which is main function of the filler material [7]. Common filler materials are for example graphite flakes or carbon nanotubes. By combining matrix and filler materials into a composite, both great mechanical strength and electrical conductivity can be achieved.

2.6.2 Metallic bipolar plates

Metallic BPPs often consist of two key components: the base metal and a coating. The most commonly used metals are steel and titanium, with the most common coatings being carbon based, titanium nitride or pure metals such as gold [12]. Metallic BPPs have great mechanical properties, with the main downsides being electrical conductivity and corrosion resistance. Due to metals having worse corrosion resistance in the PEMFC environment, corrosion in the form of oxidation may occur. Surface oxidation causes the surface contact area between fuel cells to decrease, lowering the efficiency and power output from the FC. For this reason, metallic BPPs almost always have a coating [13].

3 Theoretical background of LCA

Life Cycle Assessment (LCA) is described as a scientific approach to evaluate the environmental aspects and potential impacts associated with a process or activity [14]. The LCA concept analyses natural resource, material, and energy inputs alongside waste and emissions outputs to objectively assess a product's environmental impacts across its entire life cycle. As a globally recognised method, LCA is supported by ISO standards, notably ISO 14040:2006 and ISO 14044:2006, which define its principles, framework, and detailed guidelines. [15, 16]. According to ISO 14040, the LCA framework consists of four distinct phases: goal and scope definition, inventory analysis, impact assessment, and interpretation. Since LCA is an iterative approach, each step in LCA framework is interconnected with the earlier steps influencing the requirements on the subsequent work [17]. Figure 2 illustrates the iterative process within the LCA framework.

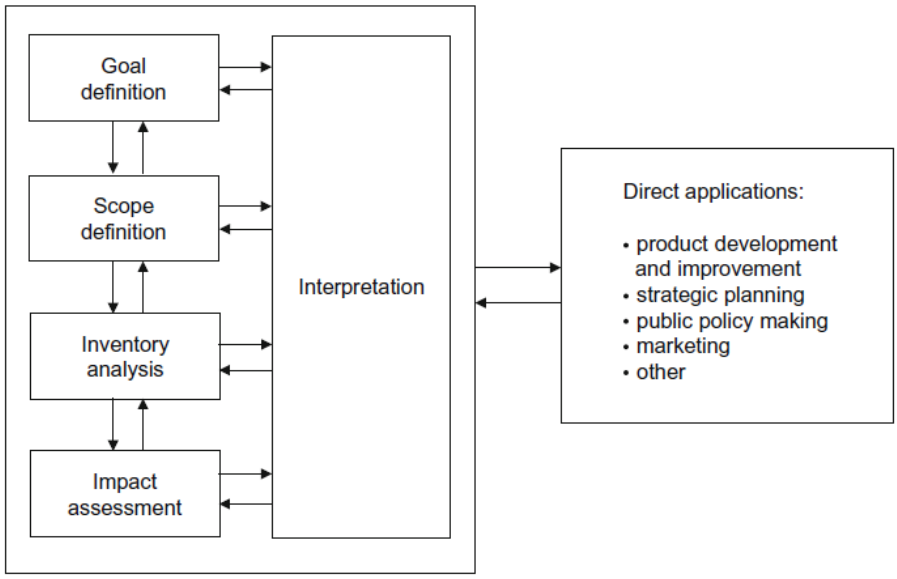

Figure 2: ISO 14040 LCA framework flowchart modified [14]

3.1 Goal and Scope Definition

The first phase of any life cycle assessment, the goal definition, is fundamental to all the other phases of the LCA process. It guides all the detailed aspects of the scope definition, such as the Intended application(s) of the results, method-related limitations, assumptions and impact coverage, reasons for carrying out the study and decision-context, and target audience of the results [17].

In LCA, the scope definition outlines the product systems to be analysed and the methods for conducting the assessment [18]. The functional unit act as one specific reference flow linking all of other modelled flows and providing the benchmark for processing the measurement of the input and output flows in the data inventory [14]. Additionally, as the basis of LCA study, a functional unit is used to be a reference point for deciding which unit processes to include and what extent they are intended to. Lastly, for a comparative LCA, the functional unit must fairly and appropriately represent the function of the systems being compared.

3.1.1 System Boundaries

The System boundaries refer to the lines that set the border between the analysed product system and the surrounding either the surrounding economy (technosphere) or the environment (ecosphere). It is important to system boundaries be presented in a diagram that provides an overview of which parts of the studied product system that are included and which are excluded. Besides, the system boundaries can be divided into four key aspects. Firstly, boundaries related to natural systems, marking where the technical system begins and ends. Secondly, geographical boundaries, identifying where the product's life cycle takes place. Thirdly, the time horizon, based on the expected lifespan of the product or system. Lastly, technical system boundaries, which may be simplified using cut-off criteria and allocation procedures.

There are two main LCI modelling frameworks: attributional and consequential LCA [14]. Attributional LCA describes the current product system, while consequential LCA assesses impacts from system changes the product may cause. For systems with bi-products, ISO 14040 recommends a hierarchy: subdivision for process detail, system expansion to include alternative functions, and allocation when others aren't feasible—ideally based on physical relationships, or economic/energy-based if needed.

3.2 Inventory Analysis

The life cycle inventory (LCI) phase involves creating a flow model with input-output data aligned to the system boundaries. Key activities include collecting primary or secondary data, ensuring data quality, and assessing environmental loads across the life cycle relative to the functional unit. The Life Cycle Inventory (LCI) phase is often the most time-consuming due to extensive data collection. This phase requires careful planning to focus effort on high-impact areas. Data quality classification by Michael et al. [14] is shown in *table 3* below.

Level	Description
Very high	Measured directly at specific process site or scaled from measurement
High	Derived from measurements at specific process site via modelling
Medium	LCI database process or data from literature specific to actual process
Low	Generic LCI database process or data from literature
Very low	Judgement by expert or LCA practitioner

Table 3: Classification of data specificity [14]

3.3 Impact Assessment

Unlike other LCA phases, LCIA is mostly automated by LCA software. According to ISO standards, mandatory steps include selecting impact categories, classification, and characterisation, while normalisation, weighting, and grouping are optional. In classification, LCI flows are sorted by impact category [4]. Impact indicators are chosen based on environmental relevance and may reflect early or late stages in the cause-effect chain [17]. *Figure 3* illustrates this framework.

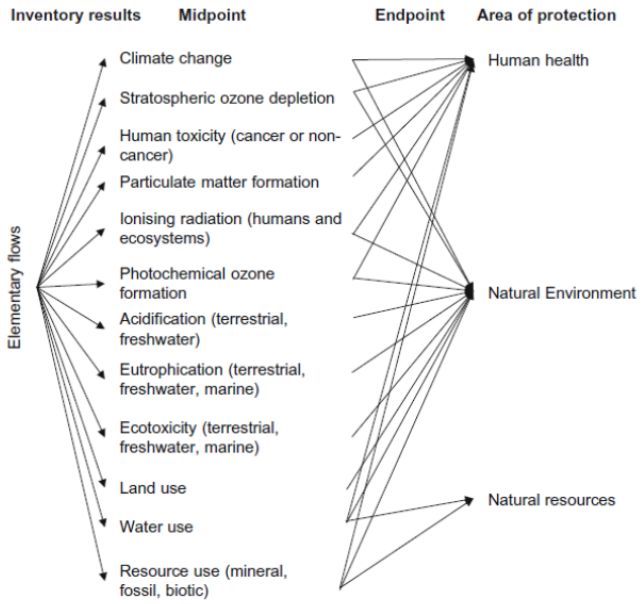

Figure 3: Framework of Impact indicators [17]

In the characterization step, elementary flows are translated into impact scores using characterisation factors (CFs), which quantify the contribution of each flow to a specific impact category based on scientific cause-effect models. Following this, the Normalization step helps to illustrate all characterized category scores relative to a common reference such as regional, global, or sectoral, making different categories easier to compare[18]. The weighting step involves assigning relative importance to impact categories using weighting factors, which helps prioritize environmental issue. Lastly, grouping further organizes impact categories into sets based on criteria such as severity or relevance.

3.4 Interpretation

The interpretation phase is the step where all of the results from previous phases are incorporated and evaluated to provide the conclusion and recommendation for the LCA study. The outcomes of this stage are discussed with respect to the study's methodology, assumptions, and limitations. The interpretation should not only be able to illustrate the results in a comprehensive way but also readable and provide clarity to ensure the audiences or study users get a clear understanding regarding the findings. As the final stage of study, interpretation should include the identification of significant issues which evaluating their impact on overall results of the study. Furthermore, completeness, consistency checks, sensitivity analysis and uncertainty analysis are also considered as the key elements on this stage to establish a significant conclusion of the LCA study. Finally, the conclusions of LCA study in this phase are presented in an iterative way based on the identification of significant issues and the key elements on the interpretation part. Recommendations are then formulated based on the conclusions and the intended application as defined in the goal definition.

4 Methodology

This section presents the overall approach taken in this study, structured into key parts: work structure, data and information gathering, detailed process descriptions of the bipolar plate production for the different materials and the calculations performed to support the life cycle assessment and scenario analysis. Each part contributes to building a comprehensive framework for evaluating and comparing the environmental impacts of the chosen materials.

4.1 Work structure

The workflow for this project was divided into six major steps, each guiding a different aspect of the analysis. These steps also reflect the structure of the following chapters in this report, providing a clear overview of how the methodology was applied:

- **Understanding the Fuel Cell System**
  A foundation was laid through general research into the working principles and structure of fuel cells, with a particular focus on the role and performance requirements of bipolar plates, as presented in Section 2.1. On top of that, performance data for both composite and metallic BPPs was gathered from literature to be used for future performance benchmarking, see *appendix C*.
- **Material Selection for Bipolar Plates**
  Various material options were evaluated for metallic bipolar plates based on performance, cost, and manufacturability to identify the most promising candidates. This is further explained in detail in section 4.4.2.
- **Defining goal and scope of the study**
  Setting the objective of the study, which is to evaluate and compare the environmental impact of bio-based BPPs with state-of-the-art and metallic BPPs, within a cradle-to-gate system boundary. This is further explained in section 5.1.
- **Mapping of Production Processes**
  Comprehensive flowcharts were developed to outline the entire production chain of BPPs from each material. Starting from raw material extraction and including the last production step of the final product, as presented in section 5.1.
- **Data Collection**
  Environmental and production data were gathered from companies as primary data and the secondary data was obtained from Ecoinvent version 3.11 [19] database. Additionally, relevant scientific literature was used to ensure reliability and completeness of the data, as further explained in section 6.4.
- **LCA Modeling and Impact Calculation**
  Life Cycle Assessment models were built for each material using openLCA version 2.3.0 [20]. The model incorporated all sub-processes and also transportation distances and modes, in accordance to the flowcharts presented in section 5.1. The impact assessment method used in this study was CML [21].
- **Result Analysis and Interpretation**
  Environmental impact results were extracted and analyzed, focusing on several impact indicators. These results are presented in section 7.2.
- **Sensitivity Analysis** Sensitivity analysis was conducted to investigate the influence of switching to locally mined graphite rather than mining in china. This sensitivity analysis testes the robustness of the results. This analysis is further explained in section 7.3.

4.2 Impact categories

This section provides a description of the impact categories relevant to the studied system.

a Global Warming Potential
The bipolar plate production system has the potential to contribute to emissions at each stage of its lifecycle. This is because energy consumption (whether from electricity or fuel) is integrated in the system. Therefore, assessing air pollutants is vital for determining the environmental impact of the system. Carbon dioxide is not the only gas which has an impact on climate change. Methane, CFCs, nitrous oxide, and other trace gases also absorb infrared radiation and thus contribute significantly to global warming. The potential contribution a substance may have on climate change is expressed as its global warming potential (GWP).

b Human Toxicity
Toxicity presents a complex impact category with various characterization methods. Typically, the toxicity category is divided into human toxicity and eco-toxicity [22]. Human toxicity potential assesses the potential harm caused by a unit of chemical released into the environment. In the lifecycle stages both of bio-based bipolar plates and SotA material bipolar plates potentially emit pollutants to the air and water, contributing to this parameter. The processes would most likely emit different amounts of pollutants. Hence, comparing them could yield valuable insight. Additionally, harmful substances are released during these processes, potentially affecting humans through exposure to emissions such as SO_2, particulate matter (PM), and other harmful substances.

c Acidification
During the raw material extraction process such as graphite mining, sulphur dioxide (SO_2) and nitrogen oxides (NOx) are released into the air. These emissions contribute to the formation of acid rain when they react with atmospheric moisture. Acid rain can then lead to acidification of soil, water bodies, and ecosystems, which can have detrimental effects on aquatic life, vegetation, and soil quality. This impact assessment quantifies acidification potential by expressing all relevant emissions in sulfur dioxide equivalents (SO_2-eq), allowing for a unified comparison of their effects.

d Eutrophication
Eutrophication refers to the excessive enrichment of nutrients, primarily nitrogen and phosphorus, in aquatic ecosystems. In the context of this LCA study, eutrophication impacts can arise from various stages of the life cycle, such as raw material extraction, manufacturing processes, transportation, and waste management.

e Ecotoxicity
Ecotoxicity is assessed using an ecotoxicological effect factor, which quantifies the change in the potentially disappeared fraction (PDF) of species in response to a change in the environmental concentration of a chemical [23]. The impact includes the effect of hazard-weighted increase in soil, freshwaters, and marine aquatic. In this LCA study, the ecotoxicity impacts are relevant due to the potential environmental hazard from the pollutants released during raw material extraction, transportation, and different production processes.

f Abiotic Depletion
Abiotic depletion potential reflects the impact of current activities on the future availability and usability of abiotic resources, such as minerals and metals [24]. Since the system boundary for the LCA study includes upstream activities such as extraction and mining of materials as well as use of fossil fuels sources, assessing this impact is relevant for understanding the potential environmental burden caused by the system.

4.3 Impact contribution of bipolar plates in the FC stack

Several research studies have investigated the environmental impact of different bipolar plate materials on fuel cell system. Three studies reported the percentage contribution in terms of global warming potential. These findings provide valuable benchmarks for understanding the relative impact of different BPP materials.

The study by Usai et al. [25], on the environmental impact of a fuel cell system for light-duty vehicles, resulted in the bipolar plates contributing to approximately 14% of the total GWP for an 80 kW fuel cell system. This study used carbon-coated titanium bipolar plates with a GWP of 0.24 kg CO_2-eq/kW.

On the other hand, Evangelisti et al. [26], using composite bipolar plates (70% graphite, 30% vinyl ester) in their life cycle assessment of PEM fuel cells for passenger vehicles, reported that bipolar plates production contributed to 20% impact of the fuel cell stack.

Furthermore, Simon and Bauer [27] projected that in a 2020 scenario, composite bipolar plates made from graphite and phenolic resin (430.4 g/kW) contributed approximately 18% of the total GWP of the fuel cell stack. The summary of bipolar plates impact contribution is presented in Table 4.

Source	**BPP Type and Composition**	**BPP Contribution to GWP**
Usai et al. [25]	Carbon-coated titanium (0.24 kg/kW_{net})	14% of FC stack GWP
Evangelisti et al. [26]	Composite (70% graphite, 30% vinyl ester)	20% of FC stack GWP
Simon and Bauer [27]	Composite (graphite and phenolic resin, 430.4 g/kW)	18.0% of FC stack GWP

Table 4: Summary of Bipolar Plate Contributions to Global Warming Potential in comparison to the entire FC stack/system

4.4 Material choice for bipolar plates

The composition of components in bio-based- and SotA composite bipolar plates were given at the start of the project with a focus on comparing the environmental impact for these materials. The choice of material for the metallic BPP was made based on literature research and a comparison of key parameters, as outlined in the following section.

4.4.1 Material composition for all composite BPPs

The material compositions for all composites were outlined in the introduction, however for greater clarity, the exact weight fraction of each component is summarized once again in Table 5.

Table 5: Weight fractions of each component for all composite bipolar plates.

Bipolar plate	Component	Weight fraction (%)
Bio	Bio-resin	20
	Graphite	80
Bio + biocarbon	Bio-resin	20
	Graphite	70
	Bio-carbon	10
SotA	Phenolic resin	20
	Graphite	80
SotA + biocarbon	Phenolic resin	20
	Graphite	70
	Bio-carbon	10

4.4.2 Metallic BPP

In this study, the material selected for the metallic bPP was stainless steel, which was based on considerations of cost, manufacturability and performance. While titanium is often used due to its excellent strength and corrosion resistance, its high cost and processing difficulty makes it less suitable for large-scale applications. Steel, on the other hand, offers good mechanical properties and is easier and more economical to manufacture. However, steel typically lacks sufficient corrosion resistance and therefore needs to be coated. The coating chosen in this case was titanium-nitrate-oxide.

After settling on steel as the material, the specific grade of steel was also considered. There are many different grades of steel, each applicable for different conditions. The most commonly used grade is 304. It is the most versatile and most widely used steel, with good corrosion resistance in most applications. Grade 316 is the most widely used molybdenum-alloyed stainless steel, ranking just behind 304 in overall importance. The addition of molybdenum significantly enhances its corrosion resistance compared to 304, especially improving its performance against corrosion in chloride-rich environments. Therefore, grade 316 is a better choice than 304 [28]. The different alloys used in making 304 and 316 stainless steels are presented in Table 6.

Table 6: The different alloys and their respective weight percentage used in making 304 and 316 stainless steel [29], [30].

Grade	Alloy Composition by Weight									
	Fe	**Cr**	**Ni**	**S**	**P**	**Mn**	**Si**	**C**	**N**	**Mo**
304	66.3-70.8 %	18-20 %	8-10.5 %	$\leq$ 0.03 %	$\leq$ 0.035 %	$\leq$ 2 %	$\leq$ 1 %	$\leq$ 0.08 %	$\leq$ 0.1 %	0 %
316	64.4-71.9 %	16-18.5 %	10-14 %	$\leq$ 0.03 %	$\leq$ 0.035 %	0 %	0 %	0 %	0 %	2-3 %

4.5 Calculations

The calculations in this project are made in order to assess the environmental impact in regards to the functional unit of 1 kW of power output. The data which would be used for the calculation only presents the active area of the bipolar plate, while the calculation needs the total area of the bipolar plate [31]. Therefore, an estimation was made by comparing the ratio between total area and active area based on values reported in the literature, as presented in Table 7. The average ratio from these sources was 2.12. Additionally, from an environmental impact standpoint, a higher ratio is more favorable.

Table 7: Values of total area and active area from literature and personal communication.

BPP material	**Total Area**	**Active area**	**Fraction**	**Source**
Composite	189	98	1.93	[32]
Metallic	567	250	2.27	[33]
N/A	103.2	48.8	2.12	[34]
Metallic	693.2	295.1	2.17	[31]

The calculations were grouped into three categories of bipolar plates: bio-based composites, SotA composites, and metallic. This means that the two bio-based composites and the two SotA composites were treated as equivalent, as their primary difference lies in the type of resin used. The results of these calculations are summarizied in Table 8. For specific details of the calculations, refer to Appendix A.

Table 8: Weight to power output for all three groups of materials

BPP material	**Weight per power output** $[kg/kW]$
SotA Composite	0.60
Bio composite	0.43
Metallic	0.34

5 Goal and Scope of the LCA study

5.1 Goal and Scope Definition

The goal of this study is equal to the aim of the project, which is to determine the environmental impact of bio-based bipolar plates and compare the results with current state-of-the-art materials for bipolar plates. Furthermore, this LCA study is conducted to provide product-specific information for the main stakeholders in the BioBPP 2 project (the consortium consists of 10 stakeholders including RISE and Volvo Group Trucks and Technology). The results of this study are also intended for audiences beyond the main stakeholders of the project, including academics, material suppliers, and automotive manufacturers.

The scope of this study will cover the cradle-to-gate life cycle stages, starting from raw material extraction and ending at the final manufacturing process of the bipolar plates. The end-of-life and use-phase life cycle stage are not included in this study due to limitations on available data. The overview of three production systems of bipolar plates are provided in the Figures 4, 5, 6 below.

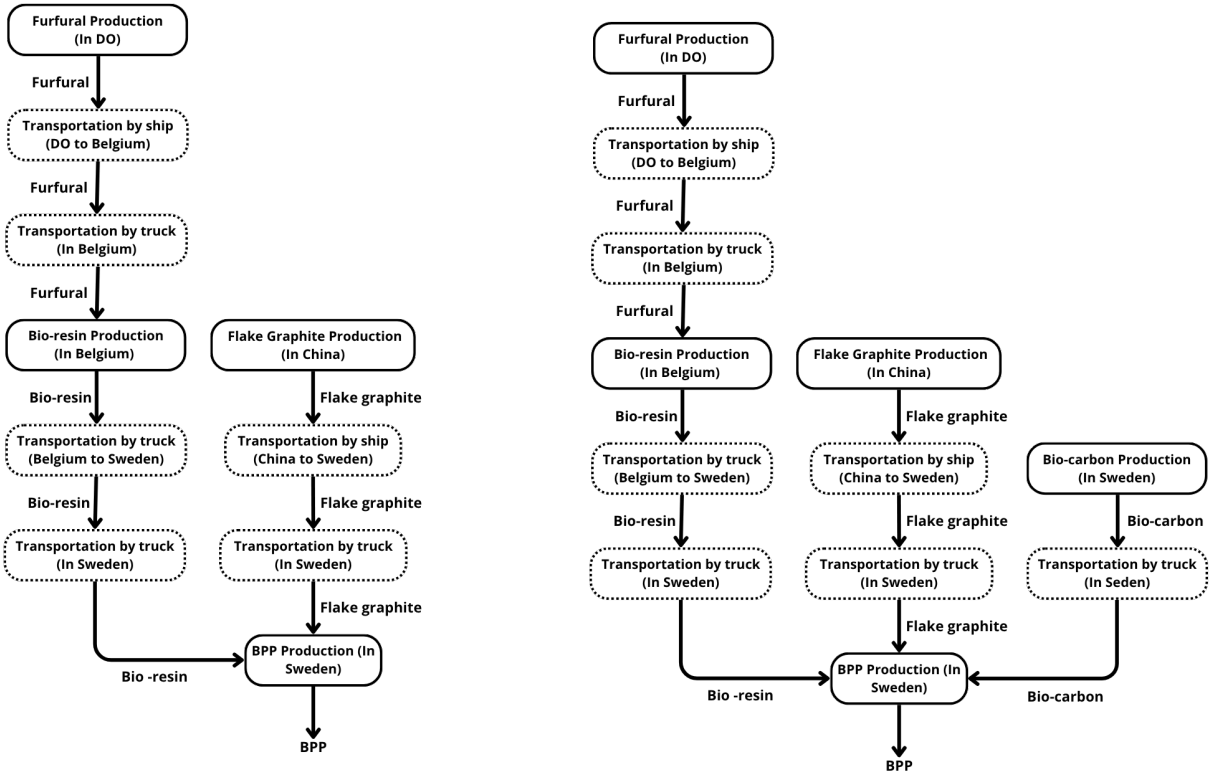

(a) Bio BPP production *(b) Bio + biocarbon BPP production*

Figure 4: Flowchart overview for bio-based composites with and without biocarbon.

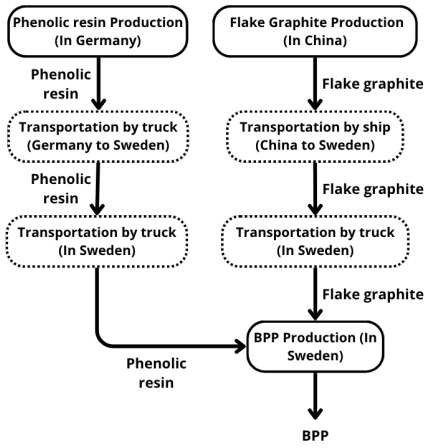

(a) SotA BPP production

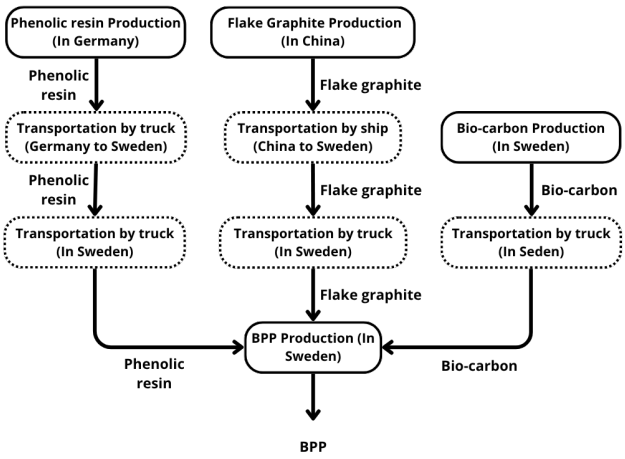

(b) SotA + biocarbon BPP production

Figure 5: Flowchart overview for SotA composites with and without biocarbon.

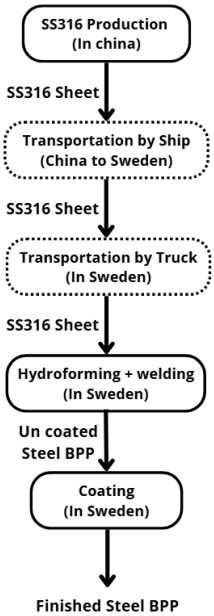

Figure 6: Flowchart overview of metallic BPP production system

5.2 Functional unit

Within the scope of this study, the system's function is to produce bipolar plates that support electrical power output in a fuel cell system. Therefore, the functional unit of this study is determined as 1 kilowatt (kW) of electrical power output from the fuel cell stack. This choice is based on the relevance of power output as the primary function of the bipolar plates within the fuel cell system. To facilitate a fair comparison among the three types of bipolar plates, the reference flow is defined as the mass (kg) of BPPs needed to produce 1 kW of power.

5.3 System boundaries

As mentioned in the background study, system boundaries can be divided into different aspects. In this section, the detail of system boundaries will be presented in relation to the natural, geographical, and temporal system boundaries.

5.3.1 In relation to natural system

The primary raw material for bio-based bipolar plates are the bio-resin and graphite, where the graphite is extracted from natural resources. Hence, the processes that require resources from a natural system is included. Furthermore, this study also considers both the emissions released to air and water as output flows to the natural system.

5.3.2 Geographical boundaries

The geographical system boundaries in this study vary based on on the data sources and locations of each step in the production process. The data for the final production process of bio-based bipolar plates and SotA composite bipolar plates is assessed using the data from activities in Sweden, while the data for the final production of metallic bipolar plates (BPPs) is primarily based on Swedish conditions, but supplemented with European average values for certain input flows. For the upstream data, such as raw material extraction and production, is set based on the location of activities. The transportation data, involves the activity of transporting materials from supplier to the site in Sweden. For long-distance or international transportation, global average data will be used, taking into account variations in fuel types, vehicle efficiency, and international shipping or aviation regulations.

5.3.3 Temporal boundaries

The current time-related boundary is used to ensure the high quality of temporal accuracy by using real time production data. This LCA focuses only on the cradle-to-gate stages, from raw material extraction up to the manufacturing process. Therefore the use phase and end-of-life impacts are outside the scope of this study.

5.3.4 Technical boundaries

Emissions from personal activities, such as commuting are not assessed in this study. Furthermore, capital goods such as equipment and infrastructure subject to changes or replacement over time—are excluded from consideration.

5.3.5 Allocation and Cut-off

The allocation procedure with physical allocation is applied in certain background data such as bagasse from sugarcane product for furfural production (raw material of bio-resin). In contrast, the production process of bipolar plates in RISE facility uses subdivision approach to separate the systems for two products (bio-based and fossil based graphite composite). Related to cut-off approach for the recycle content, This study uses the Ecoinvent cut-off system model. According to this approach, primary

production impacts are assigned to the first user of a material. Recycled materials are considered burden-free, and only the recycling process impacts are included in the secondary product system.

5.4 Type of LCA

In line with the goal of the study, the LCA is an attributional LCA which aims to compare the novel system for bipolar plate production with the current state-of-art and metallic bipolar plate productions.

5.5 Selection of impact categories

In terms of impact categories used, the study from Evangelisti et al. on LCA of fuel cell electric vehicles, incorporated global warming potential, acidification, abiotic depletion, photochemical ozone creation, and human toxicity as their key impact categories [26]. In addition to this report, a study from Lorenzo Usai et al investigated almost similar impact categories with the addition of particulate matter formation-, fossil depletion- and metal depletion potential [25]. Both studies included the environmental impact of the production of bipolar plates as a part of fuel cell systems. Therefore, selecting similar midpoint impact categories, as used in previous studies, is considered relevant for this study as well. Therfore the following impact categories were chosen: global warming potential, acidification, human toxicity, eutrophication, abiotic depletion, ecotoxicity (freshwater and terrestrial), and non-renewable energy use.

5.6 Assumptions

The following section outlines all major assumptions derived from the limitations of the study and the constraints associated with data availability.

5.6.1 General Assumptions

- Natural flake graphite without any treatment after the purification step, such as spheronization, is used as material for bio-based and SotA composite BPP [32].
- Natural graphite used is produced in China [35].
- Energy and electricity used during the production of natural graphite, assumed as China-based.

5.6.2 Bio-based BPPs

- Energy for heating during final production process is from the swedish electricity mix.
- Material loss during the final BPP production process is assumed to be negligible.
- Bio-resin production occurs in Belgium [36].
- The energy used data provided in ecoinvent data for the bio-resin production process is based on European Average.
- The production of furfuryl alcohol in Belgium is assumed to be carried out via catalytic hydrogenation [36].
- The hydrogen used in furfuryl alcohol hydrogenation process is generated via steam methane reforming (SMR), utilizing natural gas as both the feedstock and energy source. This type of hydrogen is commonly referred to as grey hydrogen [36].
- Furfural from sugarcane residue is produced in Dominican Republic using the quacker oat process [37].

- Electricity and energy used for furfural production is based on Dominican republic electricity mix.
- Bagasse, used as a raw material for furfural, has already been allocated in the dataset on a per-kilogram basis as a by-product of sugarcane production [19].

5.6.3 SotA Composite BPPs

- The manufacturing process is done by compression moulding, assumed to be similar to the final production process of the bio-based BPPs.
- The SotA composite BPPs production process is assumed to take place in Sweden.
- Phenolic resin used is assumed to have been produced in Germany [38].
- Novolac phenolic resin is assumed to be the type of phenolic resin used in the process [39].
- Electricity and energy use in phenolic resin production is estimated to follow the energy mix of Germany.

5.6.4 Metallic BPP

- The final metallic BPP production process is assumed to take place in Sweden.
- Metal working for metallic BPP is done by hydroforming [4].
- The stamping process in the ecoinvent dataset is assumed to be a suitable proxy for the hydroforming process [4].
- Titanium Nitrate Oxide is used as the coating material for the metallic BPP [4, 40].
- Stainlesss steel 316 production is located in China [41].
- Electricity and energy used in the stainless steel production process is assumed to be China-based.

5.6.5 Transportation

- Different transportation modes and distances were estimated using the Ecoinvent database, Google Maps, and several freight distance estimation websites.
- Tables 9, 10, and 11 summarize the transportation modes and distances for all transported components of the bio-based, SotA, and metallic bipolar plates, respectively. Additionally, visual representations of transportation routes are presented in section 6.

Table 9: Transportation routes, modes and distances of all components of bio-based bipolar plates.

Goods	Description	Mode	Distance (km)
Furfural	In DO	Road, Lorry	500
	From DO to BE	Sea, Bulk carrier	8000
	In BE	Road, Lorry	500
Bio resin	From BE to SE	Road, Lorry	1600
Graphite	In CN	Road, Lorry	500
	From CN to SE	Sea, Bulk carrier	17500
	In SE	Road, Lorry	500
Bio carbon	In SE	Road, Lorry	1000

Table 10: Transportation routes, modes and distances of all components of SotA composite bipolar plates.

Goods	**Description**	**Mode**	**Distance (km)**
Phenolic resin	From D to SE	Road, Lorry	1500
Graphite	In CN	Road, Lorry	500
	From CN to SE	Sea, Bulk carrier	17500
	In SE	Road, Lorry	500
Bio carbon	In SE	Road, Lorry	1000

Table 11: Transportation routes, modes and distances of all components of metallic bipolar plates.

Goods	**Description**	**Mode**	**Distance (km)**
Stainless steel 316	In CN	Road, Lorry	500
	From CN to SE	Sea, Bulk carrier	17500
	In SE	Road, Lorry	500

6 Inventory Analysis

This section describes the activity of collecting data and modelling all the processes involved in the study. Inventory analysis is presented for each type of bipolar plate and each process in the system. Primary data were exclusively obtained from the production of bio-based product and SotA composite at the RISE research facility in Sweden. The secondary data was mainly sourced from the ecoinvent datasets and relevant scientific publications. Assumptions were made in cases where specific data was not accessible. Datasets were chosen based on their geographical relevance to ensure the highest possible precision. If such datasets were not available, relevant alternatives were used instead. Additionally, all inputs and outputs for each process and material, are presented in Appendix B.

6.1 Composite BPP Production

The main production process data for both bio-based BPP (with and without bio-carbon) and SotA composite (with and without bio-carbon) were modelled based on the primary data provided by RISE. In the stirring process, raw materials (bio-resin and graphite) are mixed together before being compressed by a machine. Electricity was utilized as the primary energy source to operate equipment involved in multiple stages of the process, including mechanical stirring during material preparation, compression moulding with heating for shaping the composite materials, and subsequent testing for evaluating their properties. Each of these processes required specific electrical loads to power tools such as stirrers, hydraulic presses, and testing machines, ensuring consistent performance and reliable results throughout the manufacturing workflow. The Swedish electricity mix was used to represent the electricity supply for this process. As described in section 5.6.2 and 5.6.5, material input includes the flake graphite, which is produced and transported from china, and bio-resin which is supplied by a company from Belgium, and bio-carbon which is produced in Sweden.

6.1.1 Bio-resin Production

The life cycle inventory (LCI) for producing the bio-resin used in the bio-based bipolar plates is compiled from various sources. The process begins with bagasse, a residue from sugarcane processing, which is further processed to extract hemicellulose. Through acid hydrolysis followed by dehydration, hemicellulose is converted into furfural (F). These upstream processes take place in the Dominican Republic. The furfural is then transported by to Belgium.

As mentioned in section 5.6.2, in Belgium, furfural undergoes catalytic hydrogenation and is converted into furfuryl alcohol (FA), using grey hydrogen produced via steam methane reforming, as reported by the supplier. The FA is then polymerized through an acid-catalyzed reaction to produce polyfurfuryl alcohol (poly-FA), which constitutes the final bio-resin product. This polymerization process data, including energy inputs and output ratios, is sourced from the supplier's sustainability report [36]. After production, the bio-resin is transported to Sweden.

Most of the data regarding the furfural production, is obtained from a study by Jorge Blanco [37], while data for furfuryl alcohol production via catalytic hydrogenation are obtained from Gabriel et al. [42]. A schematic overview of the bio-resin production process is provided in Figure 7.

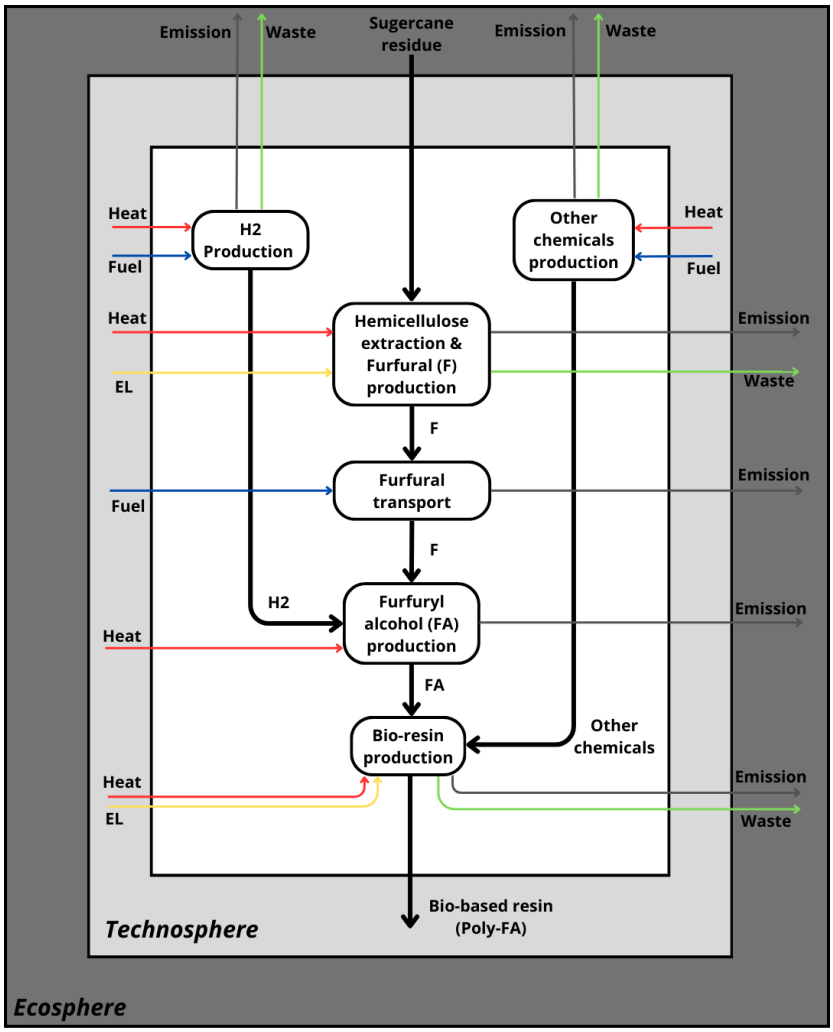

Figure 7: Flowchart of bio-resin production

6.1.2 Natural Flake Graphite Production

The type/grade of graphite used for these BPPs is natural flake graphite. The mining and production of flake graphite is assumed to occur in China, as they currently are by far the largest producer of graphite in the world. The mining is carried out using explosives and heavy machinery to extract the ore which at this step has an approximate carbon content of 11 %. After extraction, the graphite ore undergoes a process called flotation, where the ground ore is mixed with water and chemicals that cause the graphite to float to the surface, separating it from the surrounding rock. After flotation, the carbon content lies between 85 - 98 %. Additional purification steps are possible to reach the carbon content to above 99 %, however for this project only the first two steps are considered. All inputs and outputs were sourced using Eco-invent datasets [19], with the electricity and energy mix geographically adjusted to reflect the specific case of production in China. Figure **??** presents a flowchart visualizing the production processes for natural flake graphite.

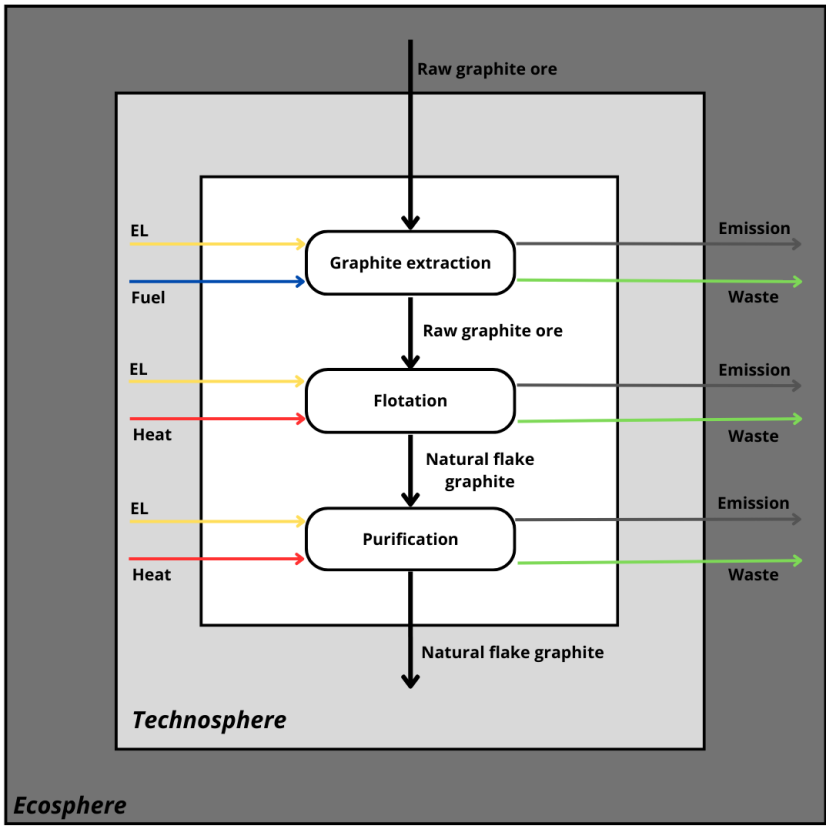

Figure 8: Flowchart of natural graphite production

6.1.3 Bio carbon production

The Swedish company Envigas supplied the biocarbon material, which has an approximately 90% C-fixation. The biocarbon is produced in Sweden by pyrolysis of forestry residue. The primary data on amount of energy use and carbon intensity per kg of product was provided directly by the company as primary data. The flow diagram of bio-carbon production is provided in the Figure 9 below.

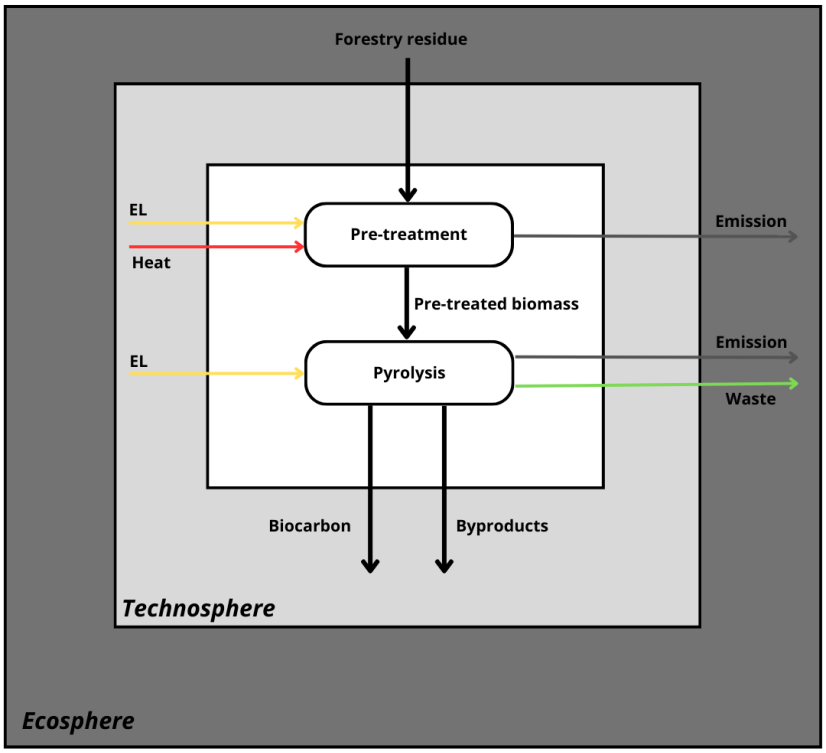

Figure 9: Flowchart of bio carbon production

6.1.4 Phenolic Resin Production

The production of phenolic resin is done through a condensation reaction of phenol and formaldehyde. Based on the use of catalyst, two types of phenolic resins can be produced. By using acid as catalyst, *Novolac* resin is produced which requires a curing agent. By instead using a base as catalyst, *Resole* resin is produced which only requires heat for curing. For this study, the phenolic resin used is Novolac resin, which is assumed to have been produced in Europe, using datasets based on multiple chemical factories in Germany. The process of phenolic resin production is shown in the Figure 10 below.

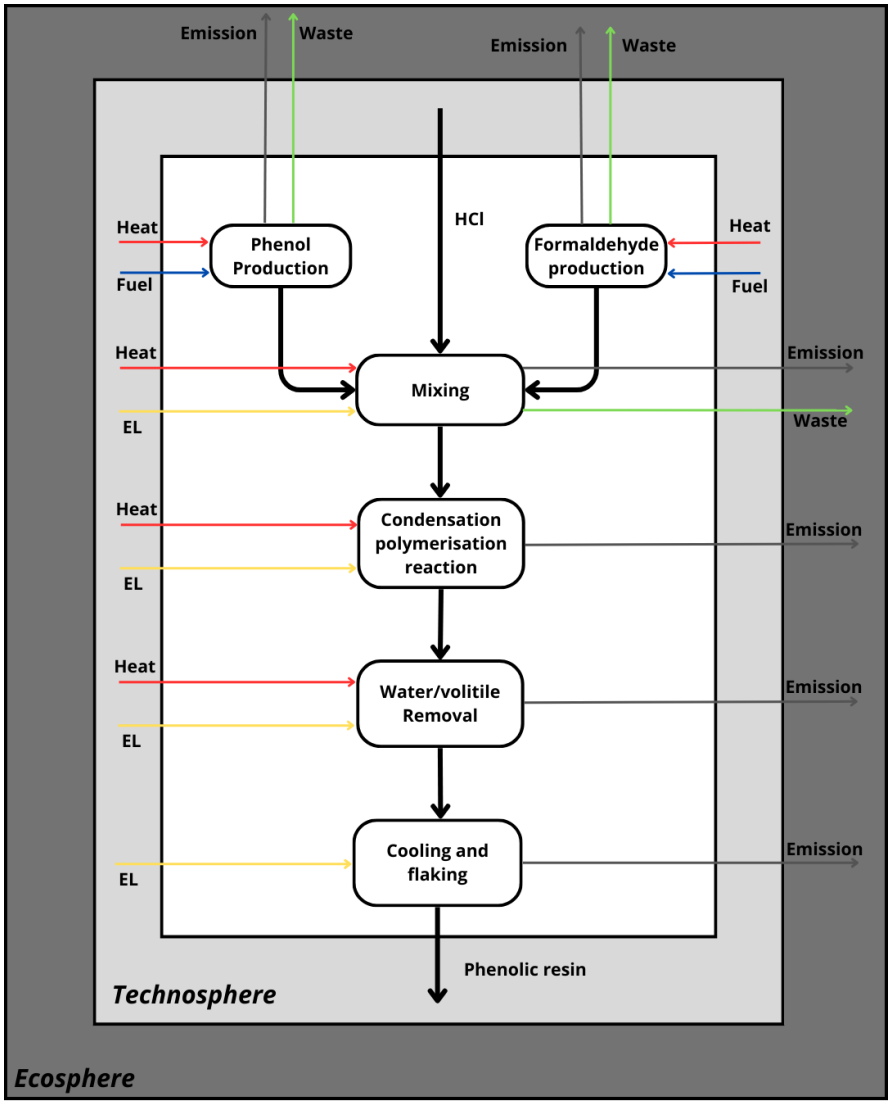

Figure 10: Flowchart of phenolic resin production

6.2 Metallic BPP Production

Since primary data for metallic BPP production were not available, this model relies on process data from the Ecoinvent database, specifically including stamping and coating steps as part of the manufacturing process. The stamping process selection follows the methodology outlined by Santesteban [4], while selective coating using titanium nitride oxide from Ecoinvent was chosen as the closest proxy to the referenced coating method [40].

As China is the largest global producer of stainless steel (SS), this study assumes that the SS 316 production takes place in China. The production process begins with the creation of pig iron by heating iron ore, coke, and limestone in a blast furnace. The resulting molten pig iron is then transferred to a basic oxygen furnace, where steel is produced. Alloying occurs in a clad furnace and the composition of alloys is presented Table 6. Alloying is then followed by continuous casting into slabs, hot rolling to thin the metal to approximately 3 mm, and finally cold rolling to achieve sheet thicknesses below 1 mm.

Due to data availability limitations, the inventory for SS 316 production is modelled using proxy data for SS 304 from Ecoinvent, with material composition adjusted based on Manan and Elsa's research [43]. Given the assumed Chinese origin of production, energy and electricity mixes are adapted to reflect Chinese conditions.

All metallic BPP manufacturing processes, including stamping and coating, are assumed to take place in Sweden, as presented in section 5.6.2. Accordingly, energy inputs for these steps are adjusted using the Swedish energy mix. It is also assumed that transportation conditions are similar to those used for graphite. One bipolar plate is composed of two halves, which are first produced through a hydroforming process, where a metal sheet is shaped against a mould using liquid pressure and then welded together to form the complete BPP. The production flow diagram of stainless 316 is provided in Figure 11.

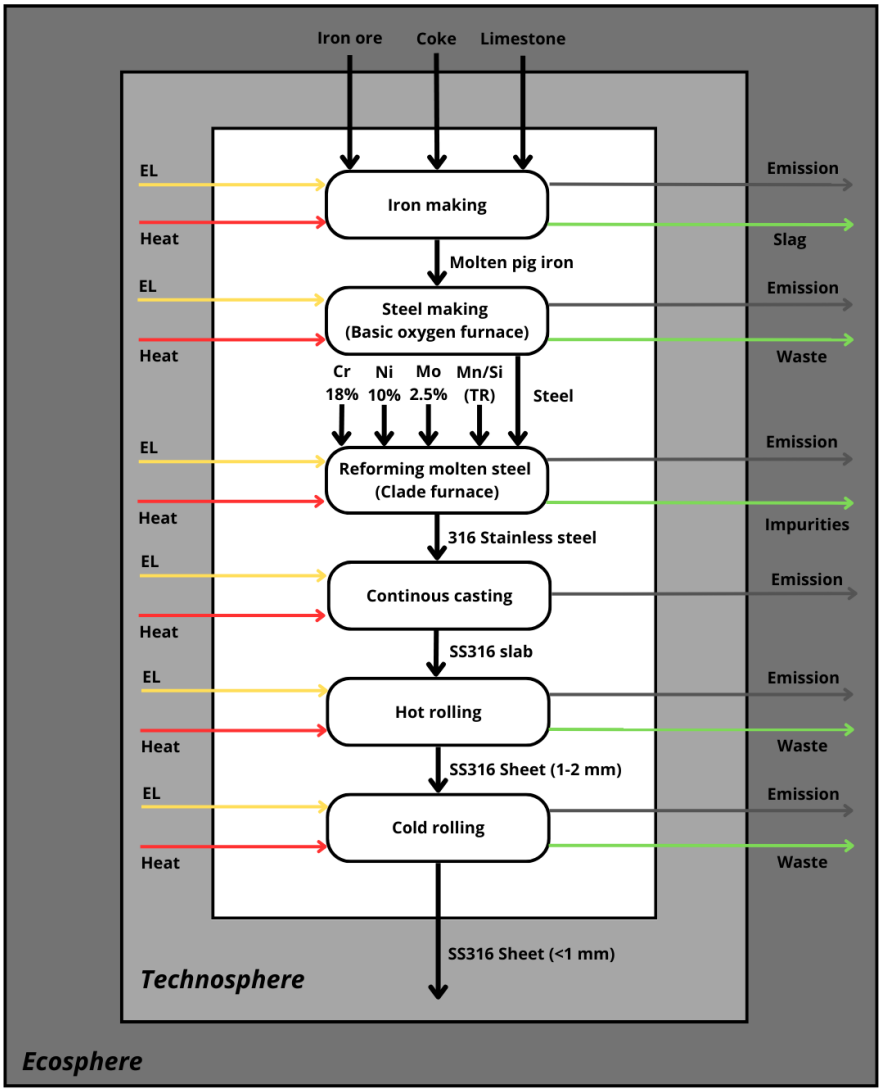

Figure 11: flowchart of stainless steel 316 production

6.3 Transportation

The transportation process is also included in this study, which are mainly the transportation of material to the manufacturing site. The transportation of flake graphite is assumed to be done by bulk cargo shipping from China to the Sweden port, then from port to RISE facility by truck. Both bio-resin and phenolic resin are supplied using long haul trucks from Belgium and Germany. The trucks with vehicle gross 16-32 tonnes were selected and EURO 6 standard was applied to meet the Swedish national regulation. As mentioned in the section 5.6.5, the distance for transportation of materials are estimated using the approximate distance from supplier location or port to the research facility.

6.4 Data Acquisition

The data used in this study consists of both primary and secondary sources. Primary data for the production of bio-based bipolar plates was collected through activities carried out in the RISE project. Background data for upstream processes was obtained from the Ecoinvent database (version 3.11), complemented by relevant scientific literature, technical data sheets, and information from company websites.

To ensure geographical relevance, country-specific average data was prioritized for each life cycle process. In cases where such data was unavailable, European or global averages were used as alternatives. While the most recent data was preferred, reliability and accuracy were given higher priority if a trade-off was necessary.

Data collection involved identifying and extracting specific values for sub-processes and material properties. These values were used as direct inputs for modelling in openLCA and for validating results against literature benchmarks, thereby enhancing the credibility of the LCA results.

7 Life Cycle Impact Assessment - Results and Interpretation

This chapter presents the results of the study including the life cycle impact assessment, interpretation of life cycle impact, and the sensitivity analysis.

7.1 Impact Assessment results comparison between all types of BPPs

In this subsection, the impact results for the bio-based bipolar plates production are compared to the SotA composite BPPs and metallic BPP. The results are presented in the Table 12 which shown the comparison for each impact.

Table 12: Comparison of LCIA results for different bipolar plate materials per 1 kW FU

Impact category	Biobased BPP	Biobased + biocarbon BPP	SotA BPP	SotA + biocarbon BPP	Metallic BPP	Unit
Acidification	1.81E-03	1.70E-03	2.82E-03	2.68E-03	3.09E-02	kg SO_2-Eq/kW
Climate change	2.55E-01	2.50E-01	5.89E-01	5.84E-01	4.12E+00	kg CO_2-Eq/kW
Eutrophication	6.15E-04	6.27E-04	1.64E-02	1.64E-02	5.22E-02	kg PO_4-Eq/kW
Human toxicity	3.91E-01	3.92E-01	7.34E-01	7.35E-01	1.52E+02	kg 1,4-DCB-Eq/kW
Material resources: metals/minerals	2.02E-06	2.07E-06	5.08E-06	5.15E-06	3.00E-03	kg Sb-Eq/kW
Ecotoxicity: freshwater	1.55E-01	1.59E-01	4.19E-01	4.24E-01	9.02E+01	kg 1,4-DCB-Eq/kW
Ecotoxicity: terrestrial	3.34E-03	3.31E-03	5.92E-03	5.89E-03	1.32E+00	kg 1,4-DCB-Eq/kW
Energy resources: non-renewable	2.91E+00	2.84E+00	1.19E+01	1.18E+01	4.36E+01	MJ/kW

7.1.1 Result interpretation of bipolar plates material comparison

This subsection presents the impact assessment results for the bio-based BPPs, state-of-the-art (SotA) composite BPPs, and metallic BPP, based on the FU of 1 kW. The results are also grouped per life cycle stage of the product, to identify the dominant contributors within each system. In addition, a hotspot analysis is provided for each impact category to support the interpretation of the findings.

a. Climate change

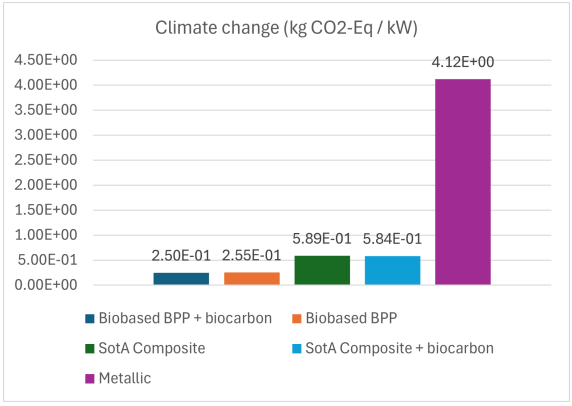

(a) Total Climate change impact comparison for all BPP materials per FU.

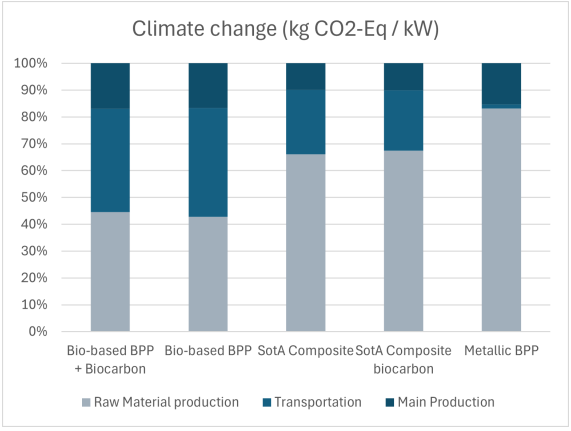

(b) Share per life cycle stage for climate change impact comparison of three BPP materials.

Figure 12: Climate Change impact comparison of different BPP materials per 1 kW functional unit.

Figure 12 illustrates the comparative contribution to climate change for the five materials. The results show a significant discrepancy among the materials. The metallic bipolar plates exhibit the highest global warming impact, with a value of approximately 12 kg CO_2-eq per FU. This is more than 12 times higher than that of the bio-based plates (0.576 kg CO_2-eq/FU) and over 10 times higher than the SotA composite material (0.987 kg CO_2-eq/FU).

Figure 12 wiich presents the percentage share per life cycle stage. These results show that the high climate change impact of metallic BPP primarily comes from the production of stainless steel as the raw material (83.1%). This is mainly due to the production of stainless steel being an energy-intensive process that in the case of China, heavily relies on electricity generated from hard coal, thereby increasing greenhouse gas emissions.

In comparison, the SotA composite BPPs also show material production as the most dominant contributor to climate change impacts. However, for the bio-based BPP, the share of material production is less significant, contributing less than 50% to the total climate change impact. This indicates a more balanced distribution of emissions across its life cycle stages, where other processes such as transportation, and main production play a relatively larger role.

For the bio-based and SotA composite BPP mixtures, the presence of bio-carbon slightly reduces the overall environmental impact compared to those of mixtures without it. This occurs because the GHG emissions from graphite production and transportation are lowered due to reducing graphite inputs in the manufacturing process. Although the production and transport of bio-carbon also generate emissions contributing to climate change, their impact is slightly smaller and can still compensate for the avoided emissions from the decreased use of graphite.

b. Acidification

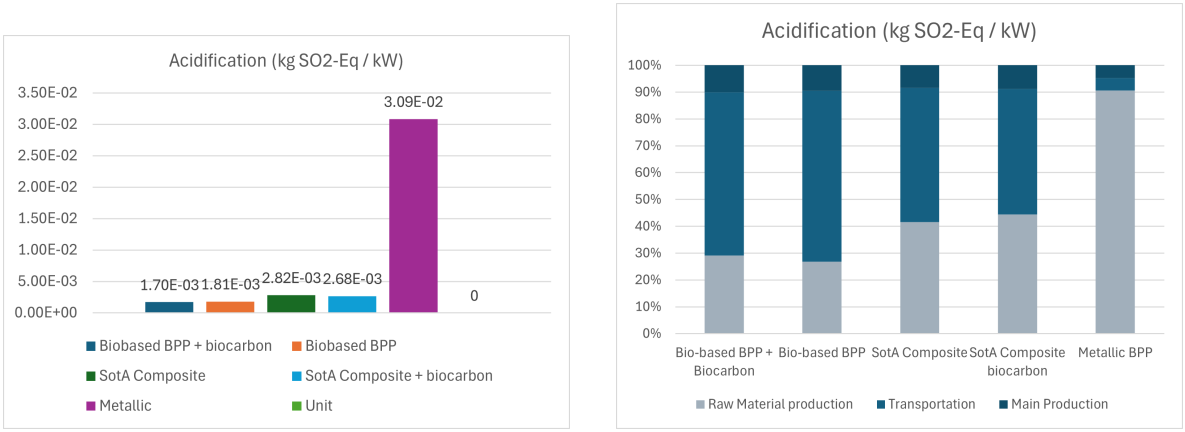

(a) Total acidification impact comparison for all BPP materials per FU.

(b) Share per life cycle stage for acidification impact comparison for all BPP materials per FU.

Figure 13: Acidification impact comparison for all BPP materials per FU.

Figure 13 presents a comparison of acidification impacts across all BPP materials. The metallic BPP has the highest impact (3.09E-02 kg SO_2-eq/FU) compared to the sota composite BPP (2.82E-03 kg SO_2-eq/FU) and bio-based BPP (1.70E-02 kg SO_2-eq/FU). The life cycle stage analysis reveals that this notable impact is primarily attributed to the production of stainless steel, particularly due to the inclusion of molybdenum. During extraction processes such as blasting, emissions of nitrogen oxides and ammonia are released, both of which contribute substantially to acidification.

On the other hand, for all composite-based BPPs, transportation processes are major contributors to acidification. These impacts arise largely from fuel combustion during long-distance freight, which emits sulphur dioxide and nitrogen oxides. This is particularly evident for the bio-based BPPs, which have the longest transportation distances for the materials and the highest impact on acidification from transportation activities among all materials (61%). The results for different

mixtures case for bio based and SotA composite BPPs also show that the acidification impact of mixtures with biocarbon have a lower impact than the mixtures without biocarbon.

c. Eutrophication

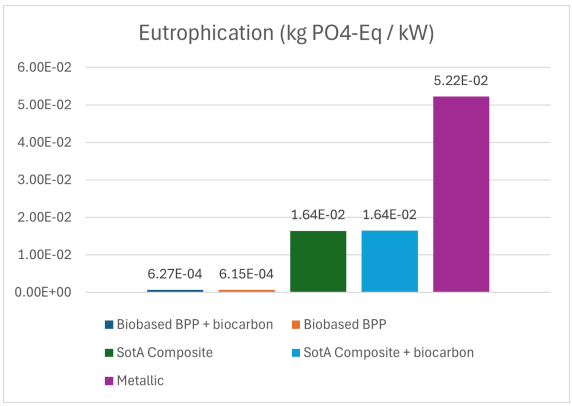

(a) Total eutrophication impact comparison for all BPP materials per FU.

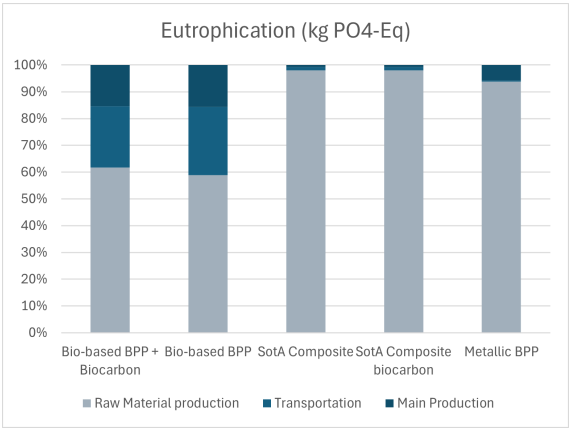

(b) Share per life cycle stage for eutrophication impact comparison for all BPP materials per FU.

Figure 14: Eutrophication impact comparison for all BPP materials per FU.

The impact on eutrophication is mainly caused by the amount of nutrients released to the environment, as explained in section 4.2). The impact from treatment of sulfidic tailing during the raw material extraction for stainless steel makes the metallic BPP have a significant impact in terms of eutrophication (5.22E-02 kg PO_4-Eq/FU). On the other hand, as shown in Figure 14, although the total impact of SotA BPPs (1.64E-02 kg PO_4-Eq/FU) is not as high as that of the metallic BPP, it should be noted that the material production stage, particularly methanol as part of phenolic resin, emits substances that contribute to eutrophication. Lastly, the eutrophication impact for the bio-based BPPs (mainly from furfural production) appears to be the lowest among them (6.27/6.15E-04 kg PO_4-Eq/FU), but it should not be neglected. In the case of the bio-based BPPs, the eutrophication impact is largely driven by upstream processes, particularly the production of furfural. While this is similar to the metallic and SotA BPPs in terms of upstream dominance, the bio-based BPP's impact appear to be more concentrated in a specific production step, as shown in section 7.2.1.

While the 10% substitution of bio-carbon leads to a slight reduction in acidification and climate change impacts for both the bio-based and SotA composite BPPs, the opposite effect is observed in the eutrophication category. In this category, the difference in impact from the two mixtures of SotA composite BPPs can be neglected. However, for the bio-based BPP, the mixture containing bio-carbon shows a slightly higher impact compared to the version without biocarbon. This increase is primarily attributed to nitrogen emissions released during bio-carbon production. Furthermore, incorporating bio-carbon does not significantly compensate for the reduction in emissions achieved by lowering the graphite content.

d. Material Resources

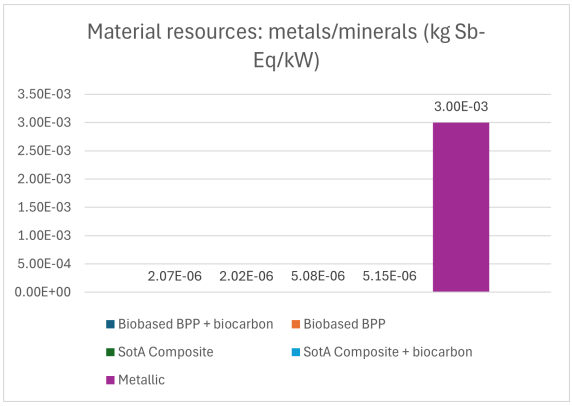

(a) Total material resources impact comparison for all BPP materials per FU.

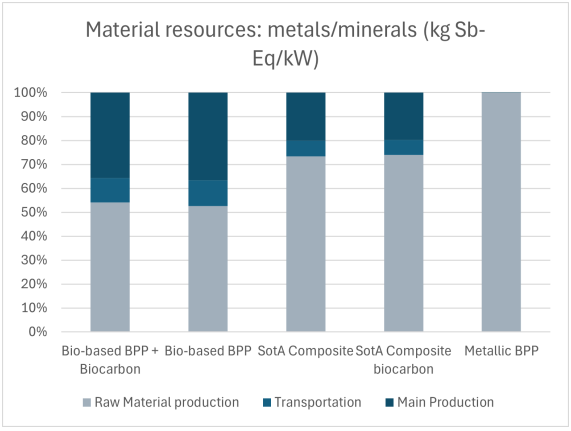

(b) Share per life cycle stage for material resources impact comparison for all BPP materials per FU.

Figure 15: Material Resources impact comparison for all BPP materials per FU.

The results in Figure 15 show that the metallic BPP has by far the highest impact compared to the other materials. Its impact value is 3.00E-03 kg Sb-Eq/FU, which is almost 600 times greater than that of the SotA composite BPPs (5.08/5.15E-06 kg Sb-Eq/FU). This significant gap is mainly due to the use of raw materials obtained from mining activities, as this impact category specifically assesses the depletion of mineral and metal resources caused by such activities. Additionally, switching from a fossil-based resin to a bio-based alternative effectively reduces the impact in this category by more than half.

The comparison among the various mixtures for both bio-based BPPs and SotA composite BPPs also shows that the mixtures incorporating biocarbon exhibit a negligible but present increase in environmental impact. This is mainly due to the inclusion of emissions from energy consumption and the energy supply system used in biocarbon production. In particular, the electricity supply contributes not only through direct emissions but also through the associated infrastructure, which involves the use of mineral resources. As a result, the impact added from biocarbon production exceeds the benefit gained from the reduction in graphite use.

e. Human Toxicity

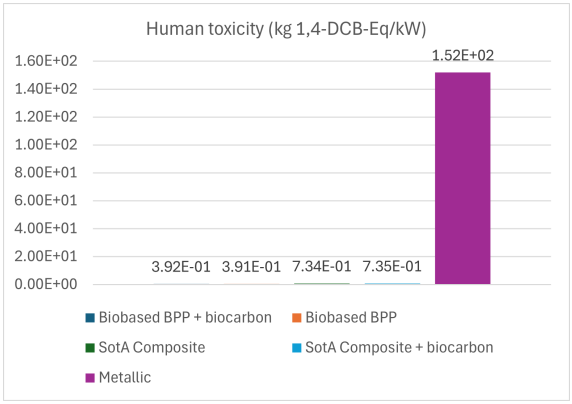

(a) Total human toxicity impact comparison for all BPP materials per FU.

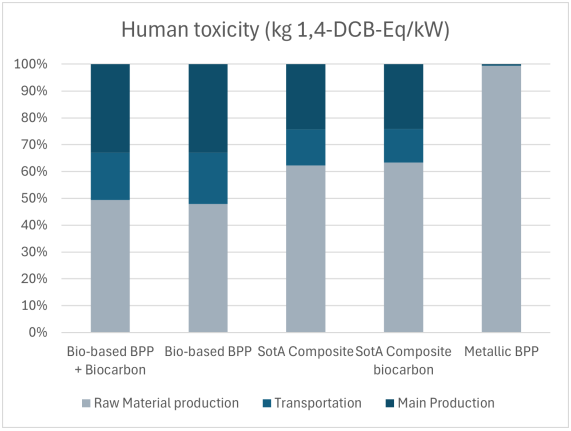

(b) Share per life cycle stage for human toxicity impact comparison for all BPP materials per FU.

Figure 16: Human toxicity impact comparison for all BPP materials per FU.

The human toxicity impact shows a very large difference between the three BPP groups. The metallic BPP has the highest value, reaching 152 kg 1,4-DCB-eq/FU, while bio-based and SotA composite BPPs have much lower values at 0.392 and 0.734 kg 1,4-DCB-eq/FU, respectively.

This large gap is mainly caused by the amount of heavy metals released in the mining and processing of metals such as molybdenum. These activities release harmful substances into water, which greatly increases the human toxicity score. However, the bio-based and SotA composite BPPs do not include significant heavy metal mining, so their toxicity levels are much lower. Their impacts come mostly from the production of chemicals and transportation, which have smaller effects in this category.

As shown in the results, the influence of bio-carbon material as a 10% substitution for graphite creates a minor difference between the mixtures for both the bio-based and the SotA composite BPPs. The mixture containing bio-carbon shows a 0.25% higher impact in this category for both groups of BPPs. This impact is due to the energy inputs involved in bio-carbon production, which generates pollutants such as SO_2 and particulate matter (PM) during the upstream process.

f. Freshwater and Terrestrial Ecotoxicity

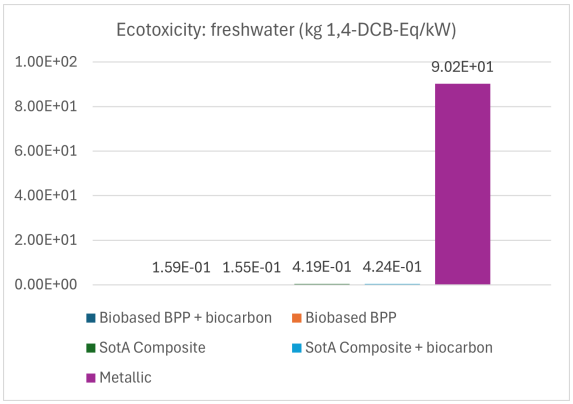

(a) Total freshwater ecotoxicity impact comparison for all BPP materials per FU.

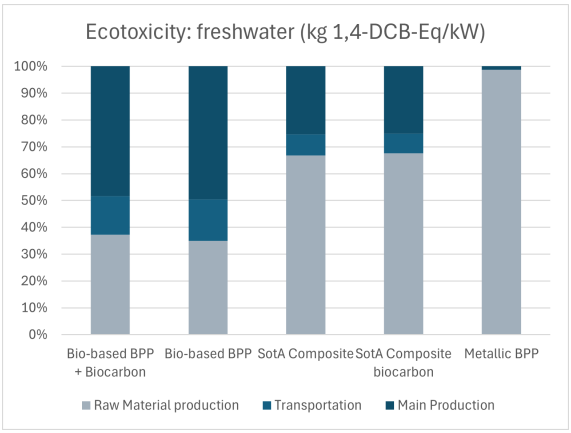

(b) Share per life cycle stage for freshwater ecotoxicity impact comparison for all BPP materials per FU.

Figure 17: freshwater ecotoxicity impact comparison for all BPP materials per FU.

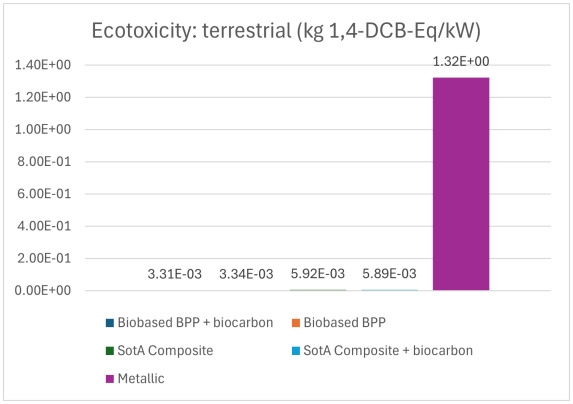

(a) Total terrestrial ecotoxicity impact comparison for all BPP materials per FU.

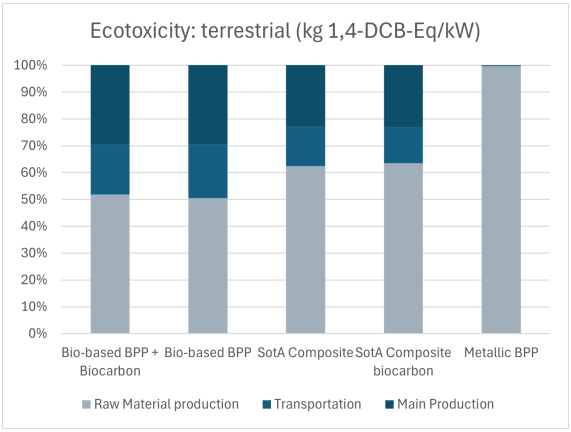

(b) Share per life cycle stage for terrestrial ecotoxicity impact comparison for all BPP materials per FU.

Figure 18: Terrestrial ecotoxicity impact comparison for all BPP materials per FU.

As shown in Figures 17 & 18, the impacts of freshwater ecotoxicity and terrestrial ecotoxicity per functional unit are also dominated by the metallic BPP system, with values of 9.02E+01 kg 1,4-DCB-Eq/FU and 1.32E+00 kg 1,4-DCB-Eq/FU, respectively. The SotA composite BPPs show the second highest impacts 4.19E-01 kg 1,4-DCB-Eq/FU and 5.92E-03 kg 1,4-DCB-Eq/FU. The bio-based BPPs exhibit the lowest impacts, 1.59E-01 kg 1,4-DCB-Eq/FU and 3.31E-03 kg 1,4-DCB-Eq/FU). This trend is similar to that observed in the human toxicity category, where the metallic BPP also has significantly higher impacts than the composite alternatives. The main reason for these substantial impacts is that all three toxicity-related categories in the metallic BPP are primarily influenced by the release of toxic substances into the environment during mining activities.

It is also worth to note that, in the freshwater ecotoxicity impact category, the percentage share of the total impact for the bio-based BPPs is dominated by the main production activity and transportation of materials (52% in total).

For both ecotoxicity impacts, freshwater and terrestrial ecotoxicity, the main contributors are mainly from toxic pollutants such as heavy metal, which are released to water body (freshwater) or soil (terrestrial). As a result, the bio-based BPP and SotA composite containing bio-carbon exhibit a slightly lower impact in these categories, primarily because of the energy inputs in the upstream processes of the systems.

g. Energy Resources: Non-renewable

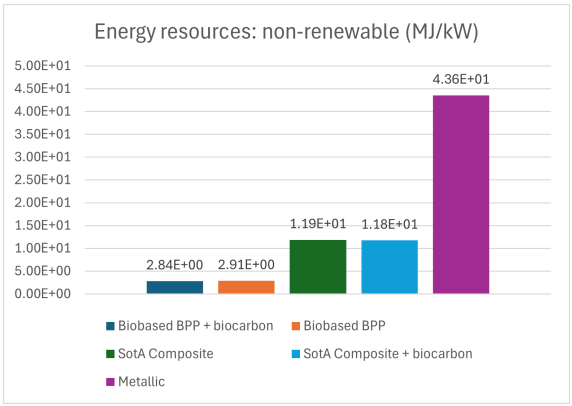

(a) Total energy resources impact comparison for all BPP materials per FU.

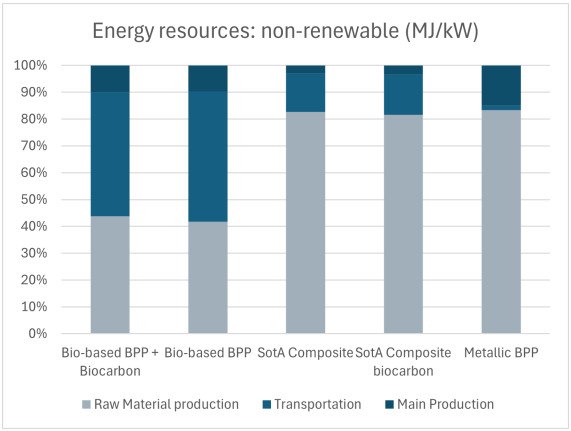

(b) Share per life cycle stage for energy resources impact comparison for all BPP materials per FU.

Figure 19: Energy resources: Non-renewable impact comparison for all BPP materials per FU.

As shown in Figure 19, the impacts associated with non-renewable energy resource use vary significantly among the materials. The metallic BPP, , exhibits the highest impact at 4.36E+01 MJ/FU, primarily due to stainless steel production. The SotA composite BPPs follow with an impact of 1.19E+01 MJ/FU, while the bio-based BPP shows the lowest impact at 2.84E+00 MJ/FU.

Since this category reflects the depletion of non-renewable resources caused by material and energy use, both the metallic and SotA composites contribute significantly to non-renewable resource reduction in the long term. This is mainly due to the energy-intensive production of their components materials. In contrast, the non-renewable energy use in the bio-based BPPs is more evenly distributed across their life cycle stage. Transportation phase, which relies heavily on fossil fuels, accounts for 46% of their impact, while material production contributes around 44%, indicating a more balanced distribution of impact sources.

In this category, the substitution of bio-carbon in the mixture results in a lower impact for both the bio-based and SotA composite BPPs. This is because the use of bio-carbon reduces the environmental burden associated with graphite mining, which is a significant contributor to the abiotic depletion potential.

7.2 Hotspot analysis for bio-based BPPs with biocarbon

In this sub-section, the LCIA results are presented as two parts. First, the environmental impacts associated with the life cycle of bio-based bipolar plates, including a breakdown of individual process contributions. Then an interpretation of how each stage affects the overall impact will be presented.

The impact calculations applied the midpoint method of the CML IA impact assessment framework [21]. The process impact results presented here are based on the scenario of the bio-based BPP composition, in which 10% of the graphite is substituted with biocarbon. This particular mixture was chosen for the assessment because it involves more processing steps compared to other bio-based BPP mixtures, making it more representative of the system's complexity.

In this method, some impact categories use different terminology, such as climate change for global warming potential, material resources: metals/minerals for abiotic depletion potential, and energy use: non-renewable for the abiotic depletion: fossil fuel. However, the characterisation indicators remain consistent with those described in the methodology section of this study. Furthermore, it is worth noting that the impact assessment of this study does not involve the normalisation and weighting step to avoid introducing subjective or region-specific preferences into the interpretation of LCA results.

The total impact assessment results per functional unit for the entire life cycle of these bio-based bipolar plates are presented in Table 13, while Table 14 shows the results for all the major processes included in the system boundary. The results cover impact categories and reflect the contribution of the main processes within the system boundary.

Table 13: Biobased BPP with biocarbon impact assessment results by category per 1 kW FU

Name	**Impact result**	**Unit**
Acidification	1.70E-03	kg SO_2-Eq/kW
Climate change	2.50E-01	kg CO_2-Eq/kW
Eutrophication	6.27E-04	kg PO_4-Eq/kW
Human toxicity	3.92E-01	kg 1,4-DCB-Eq/kW
Material resources (metals/minerals)	2.07E-06	kg Sb-Eq/kW
Ecotoxicity (freshwater)	1.59E-01	kg 1,4-DCB-Eq/kW
Ecotoxicity (terrestrial)	3.31E-03	kg 1,4-DCB-Eq/kW
Energy resources (non-renewable)	2.84E+00	MJ/kW

Table 14: Impact from each process within the bio BPP system, based on the functional Unit of 1 kW.

Process	A	CC	E	HT	MR	EF	ET	ER
Graphite Production	7.30E-05	1.22E-02	2.48E-05	1.28E-02	1.83E-08	6.08E-03	4.01E-05	1.17E-01
Transportation of Graphite (CN-SE)	8.00E-04	3.77E-02	8.74E-05	3.05E-02	4.61E-08	8.27E-03	3.62E-04	4.59E-01
Transportation of Graphite (SE)	5.94E-05	3.07E-02	2.38E-05	1.98E-02	8.98E-08	7.63E-03	1.15E-04	4.59E-01
Bio resin Production	3.29E-05	1.37E-02	8.25E-06	3.61E-03	7.07E-09	1.64E-03	3.11E-05	1.94E-01
Transportation of Bio resin (BE-SE)	2.72E-05	1.40E-02	1.09E-05	9.03E-03	4.11E-08	3.49E-03	5.25E-05	2.10E-01
Furfuryl alcohol Production	2.59E-05	3.73E-02	1.42E-05	6.78E-03	4.07E-08	3.80E-03	5.60E-05	4.44E-01
Furfural Production	3.43E-04	4.39E-02	3.11E-04	1.62E-01	9.93E-07	4.17E-02	1.55E-03	4.41E-01
Transportation of Furfural (DO-BE)	1.35E-04	6.28E-03	1.51E-05	4.97E-03	1.42E-08	1.25E-03	5.56E-05	7.66E-02
Transportation of Furfural (BE)	9.42E-06	4.86E-03	3.77E-06	3.13E-03	6.96E-09	1.21E-03	1.82E-05	7.28E-02
Compression Molding	1.71E-04	4.24E-02	9.62E-05	1.29E-01	7.40E-07	7.68E-02	9.81E-04	2.86E-01
Bio carbon Production	2.14E-05	4.28E-03	2.85E-05	8.37E-03	6.24E-08	5.93E-03	4.04E-05	4.80E-02
Transportation of Bio carbon (SE)	5.35E-06	2.67E-03	2.71E-06	1.58E-03	1.18E-08	8.44E-04	9.43E-06	3.58E-02
Total Impact	1.70E-03	2.50E-01	6.27E-04	3.92E-01	2.07E-06	1.59E-01	3.31E-03	2.84E+00

Abbreviations: A = Acidification [kg SO_2-eq/kW], CC = Climate change [kg CO_2-eq/kW], E = Eutrophication [kg PO_4-eq/kW], HT = Human toxicity [kg 1.4-DCB-eq/kW], MR = Material resources: metals/minerals [kg Sb-eq/kW], EF = Ecotoxicity: freshwater [kg 1.4-DCB-eq/kW], ET = Ecotoxicity: terrestrial [kg 1.4-DCB-eq/kW], ER = Energy resource: Non-renewable [MJ/kW].

The results show a variety of impacts caused by the processes in the system. As the main process does not involve direct emission to the environment, impacts from compression moulding process is aggregated by grouping the impacts from electricity and material inputs. A detailed explanation, including dominance analysis, is provided in the following interpretation section.

7.2.1 Contribution analysis of process impact for bio-based BPPs

A contribution analysis was carried out based on the results from table 14. Figures 20 & 21 indicate that the environmental impacts are not concentrated in one single life cycle stages, but rather distributed across the group of processes.

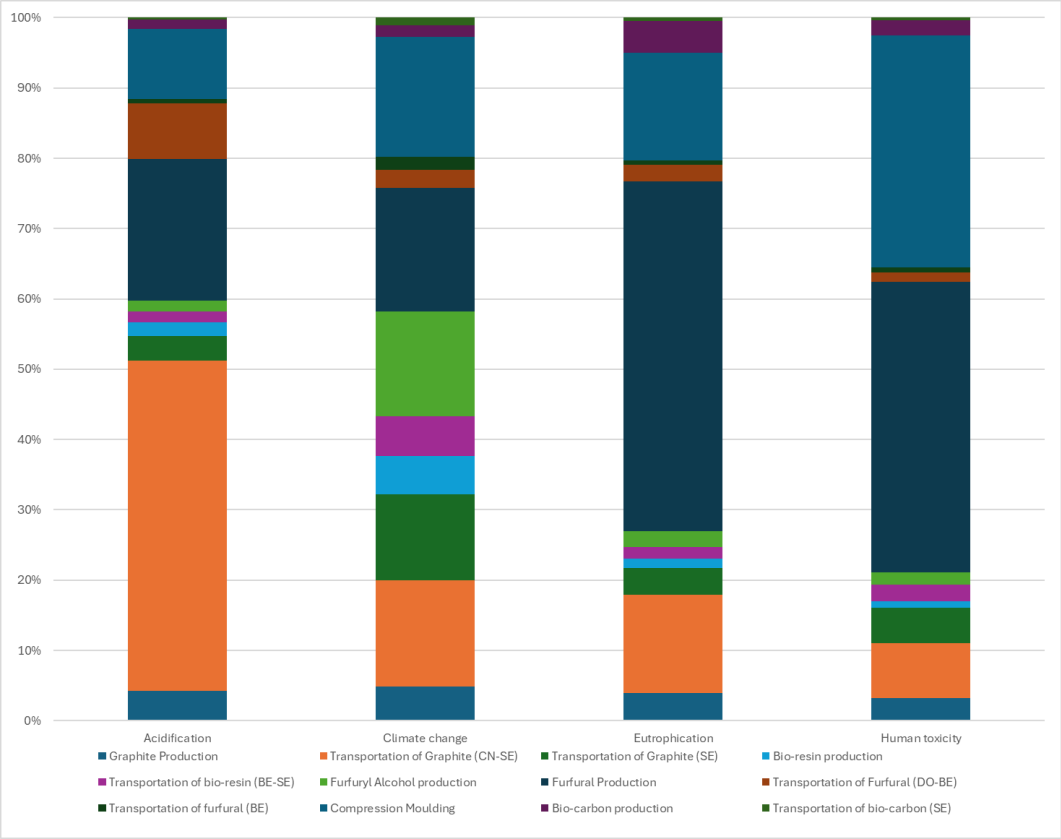

Figure 20: Process Impact Assessment of bio-based BPP: Acidification, Climate Change, Eutrophication, and Human Toxicity per FU

The compression moulding, which is the main manufacturing step of bipolar plates, demonstrates significant impacts across all indicators with each category showing more than 10% impact. This process is also identified as the largest contributor in freshwater ecotoxicity (48.5%), and becomes the second most impactful phase in climate change (16.99%), eutrophication (15.36%), human toxicity (32.95%), mineral resources depletion (35.76%), and terrestrial ecotoxicity (16.99%). Upon closer examination, these notable impacts are attributed to the electricity inputs required for the process, which are derived from various fuel sources, including a small portion from natural gas power plants.

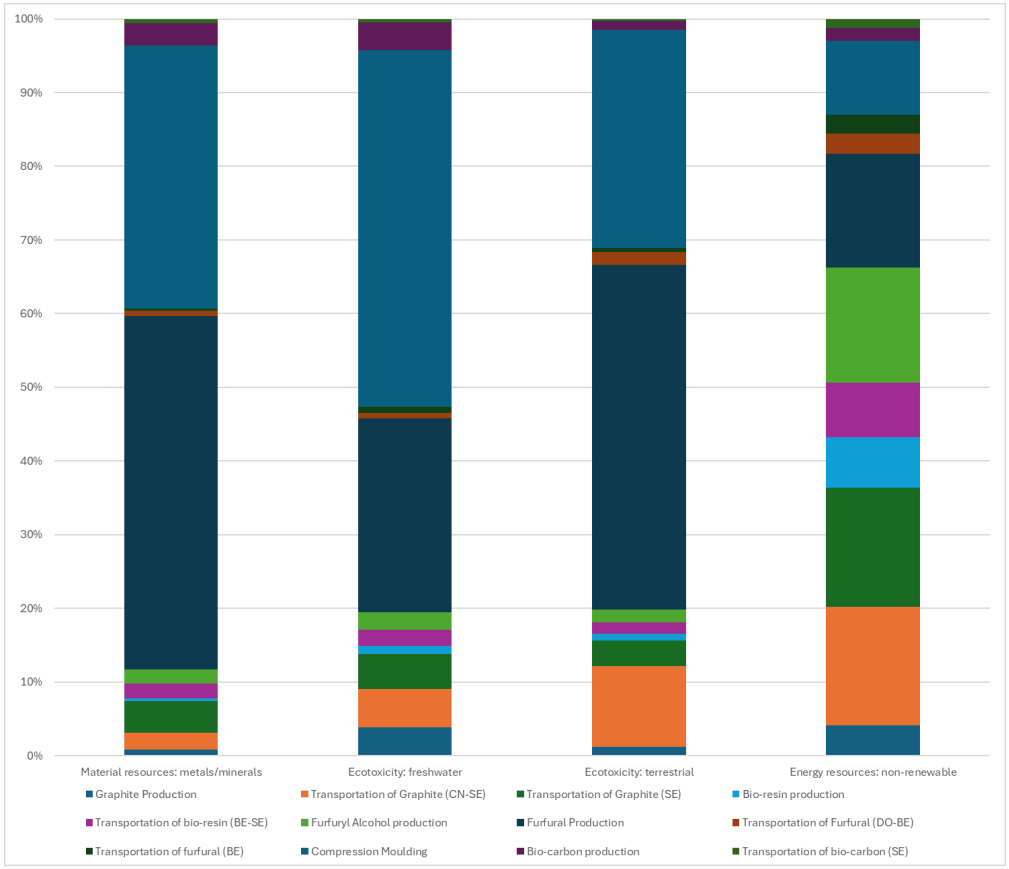

Figure 21: Process Impact Assessment of bio-based BPP: Material resources:metal/minerals, ecotoxicity:fresh water, ecotoxicity: terrestrial, energy resources: non-renewable per FU

In addition to the core process, the transportation stages also have significant impact across several categories. The long distance shipment of natural flake graphite from China to Sweden accounts for 46% of the acidification potential, making it as the most dominant process in that category. This transportation also becomes among the top three contributors to climate change (15.08%), eutrophication (13.97%), and non-renewable energy use (16.14%). The environmental impacts of this process are mainly caused by emissions from heavy fuel oil, either during its production or its use in transportation. Similarly, international transportation of furfural from the Dominican Republic to Belgium also creates significant impact, particularly in acidification (7.95%). Even regional transport activities within Europe, such as the delivery of graphite within Sweden and furfural within Belgium, show non-negligible contributions in energy- and emission-related categories.

Moreover, among material production processes, furfural production stands out as a hotspot in several impact indicator such as eutrophication (49.7%), human toxicity (41.4%), and terrestrial ecotoxicity (46.8%). These impacts are driven by the chemical and energy-intensive nature of the process, which relies on a fossil fuel-dominated electricity mix. Furfuryl alcohol production also contributes notably to climate change (14.94%) and non-renewable energy depletion (15.50%), with the impacts primarily arising from grey hydrogen and electricity inputs used during the process. Since grey hydrogen is typically produced from natural gas via steam methane reforming, it is associated with high greenhouse gas emissions, making it a major contributor to the environmental burden of furfuryl alcohol synthesis.

7.3 Sensitivity analysis

The sensitivity analysis focused on the sourcing of natural graphite. Specifically, the extraction location, which was shifted from China to Sweden to reflect a future scenario in which graphite mining and extraction becomes available domestically in Sweden. Similar to the reasoning behind choosing the bio-based BPP with bio-carbon substitution (70% graphite, 10% bio-carbon, 20% bio-resin) for the process impact analysis, in this sensitivity analysis, the same product composition is used as the baseline case LCIA due to the complexity of the process system. The results for the sensitivity analysis are presented in Table 15, showing both the updated environmental impact values and the percentage change.

Table 15: Sensitivity analysis results for natural graphite mining in Sweden, for the bio BPPs with biocarbon

Impact indicator	**Baseline LCIA Result**	**Sensitivity Analysis Result**	**Impact Change**	**Change (%)**
Acidification (kg SO_2-Eq/kW)	1.70E-03	8.65E-04	-8.38E-04	-49.2%
Climate change (kg CO_2-Eq/kW)	2.50E-01	2.04E-01	-4.56E-02	-18.3%
Eutrophication (kg PO_4-Eq/kW)	6.27E-04	5.25E-04	-1.02E-04	-16.3%
Human toxicity (kg 1,4-DCB-Eq/kW)	3.92E-01	3.53E-01	-3.84E-02	-9.8%
Material resources: metals/minerals (kg Sb-Eq/kW)	2.07E-06	2.02E-06	-4.64E-08	-2.2%
Ecotoxicity: freshwater (kg 1,4-DCB-Eq/kW)	1.59E-01	1.47E-01	-1.18E-02	-7.4%
Ecotoxicity: terrestrial (kg 1,4-DCB-Eq/kW)	3.31E-03	2.94E-03	-3.76E-04	-11.3%
Energy resources: non-renewable (MJ/kW)	2.84E+00	2.30E+00	-5.38E-01	-18.9%

As shown in Table 15, sourcing graphite from Sweden leads to a notable reduction in environmental impact across all indicators, except for material resources: metals/minerals. The three indicators with the greatest percentage decreases were acidification, energy resource: non renewable use, and climate change. In particular, for the acidification category in the baseline case LCIA result, transporting graphite from China accounts for 46.94% impact, which is primarily due to direct emission of SO_2 and NO_x generated from the heavy oil fuel used during shipping. Furthermore, the energy use during the extraction of graphite in China contributes another 4.28% impact by releasing the same substance into the environment. As a result, the shifting of graphite sourcing location leads to an acidification impact reduction of 49.2%.

Furthermore, the climate change impact shows an 18.3% reduction, mainly due to the elimination of GHG direct emissions of fuel used in the international shipping (previously 15.07%) and the substitution of China's energy-intensive production process (4.88%). More detail about the contribution impact from each process can be seen in Section 7.2.1. In conclusion, shifting to a local graphite source in Sweden can potentially eliminate the high-impact from long haul transport step and energy used in China, significantly reducing the environmental burden and positively influence the overall system impact.

8 Discussion

In this chapter, the results from the life cycle assessment is discussed in more detail. The focus is on understanding the main reasons behind the environmental impacts of each material. The discussion also considers the limitations of the study, especially the lack of primary data—and how this affects the reliability of the results. Finally, some ideas for future improvements and further research are disscused.

8.1 Life Cycle Assessment

8.1.1 Comparison of BPP materials

Based on the current results, bio-based BPPs show significantly lower environmental impacts across all assessed categories when compared to state-of-the-art composite and metallic BPPs. However, this comparison must be interpreted with caution. While all materials rely primarily on secondary data, the data quality differs as the production processes for SotA composite and metallic BPPs are well-established and thoroughly documented, making the data more reliable. In contrast, the processes for producing bio-based BPPs are less mature and not widely standardised, which means the available data is less robust and potentially more uncertain. Therefore, to improve the reliability of the comparison, more primary data on the bio-based BPP production processes is needed. This need for further data collection is discussed in greater detail in Section 8.3.

Metallic BPPs exhibited by far the highest impacts across all environmental indicators. As shown by the calculations, they also have a significantly lower weight per unit of power output. However, even so, metallic BPPs continue to show higher impacts across all indicators. This is primarily due to the numerous energy- and electricity-intensive processes involved in stainless steel production. Notably, the production of stainless steel sheets alone accounts for approximately 80–90% of the total climate change impact. However, it is important to mention that the impacts from metallic BPP production are also very high due to the type of LCA method chosen. If the end-of-life phase had been included, different results might have been obtained, as most metals can be recycled while composites currently cannot.

As previously noted in Section 5.6.5, the most significant limitation of this study is the lack of primary data. This issue becomes particularly critical when assessing novel technologies, where data gaps often require numerous assumptions. Although these assumptions are informed by existing literature, the available sources predominantly reflect state-of-the-art or well-established processes. As a result, they may not accurately represent the characteristics or performance of emerging technologies such as bio-based BPPs.

8.1.2 Hotspot analysis of biobased BPP with biocarbon

For bio-based bipolar plates, the production of furfural is the dominant contributor to climate change and most other environmental impact categories. This is largely due to the high energy and electricity demands of the process, which takes place in the Dominican Republic. Given the region's coal-dominated electricity mix, significant environmental impacts are to be expected. The compression moulding process also has a high impact on most environmental indicators due to its substantial electricity consumption.

Two other major contributing processes are the transportation of graphite, both by ship from China to Sweden and by truck within Sweden. Although bulk carriers typically have relatively low environmental impact due to their ability to transport large volumes, the vast distance between China and Sweden results in considerable emissions. In total, transportation accounts for nearly 40% of the total climate change impact. While this figure is quite high, it is understandable

given that the two main components of the bio-based BPP originate from opposite sides of the globe and require multiple intermediate transportation steps.

8.1.3 Potential GWP reduction in the fuel cell stack from bio-based BPP implementation

In this study, the biobased bipolar plates demonstrated substantially lower global warming potential compared to both composite and metallic BPPs. Specifically, the bio-based BPPs showed approximately 58% lower GWP compared to SotA composite BPPs (0.250 $kgCO_2eq/FU$ vs. 0.589 $kgCO_2eq/FU$). When applying this difference to the context of Simon and Bauer's study [27], where the composite BPP accounted for 18% of the GWP for the fuel cell stack, the bio-based BPPs would result in a 10.4 % GWP redution of the fuel cell stack.

Furthermore, when comparing the results to the study by Evangelisti et al. [26], BPPs accounted for approximately 20 % of the GWP for the FC stack. Hence, by implementing bio-based BPPs instead of SotA composite BPPs, a 11.6 GWP reduction of the FC stack can be achieved, assuming the environmental impacts from all other components in the system remain unchanged.

These comparisons, while insightful, should be interpreted with caution due to differences in system design, material composition, and scale across studies. Nonetheless, the results illustrate the promising potential of bio-based BPP to improve the sustainability of fuel cell technologies.

8.2 Performance matrix

As mentioned in research question 3 under Section 1.2, the performance matrix was initially intended to compare all materials considered for bipolar plates. The primary objective, however, was to evaluate the novel bio composite against the current state-of-the-art composite, as this would provide the most equitable comparison due to their similar material characteristics and composition. Additionally, steel was also included to offer broader context and a more comprehensive perspective on overall performance. However, due to the bio composite still being in the testing phase and the time frame of the project being limited, this objective was changed to instead researching performance benchmarks for SotA and metallic BPPs to be compared against when the performances of bio BPPs are determined. This performance benchmarking is found in appendix C.

It is important to mention that a performance comparison between the SotA composite BPPs and steel BPP is not as relevant. As shown in Table 19, literature on each material rarely focuses on the same performance parameters. The reason behind this occurrence is the fact that these materials have different limitations and are therefore tested on different performances. For example, a steel BPP does not have any permeability or flexural difficulties. Hence, Steel BPPs will not be tested on these performances. However, steel does have challenges when it comes to corrosion, which is why data on this performance is easily available. As for composite BPPs, these often have difficulties with permeability and especially flexural strength, which is why much data on this is available. On the other hand, composite BPPs do not have challenges with corrosion and therefore no data is found on this.

8.3 Future work

As previously mentioned, the bio-based BPPs are currently in an early testing phase, and more comprehensive performance data is expected to become available in the near future. Therefore, a key improvement to this work would be to include a detailed performance comparison between the state-of-the-art composite and the bio-composite. Additionally, to get more accurate life cycle impact results for the different materials, all parts of the BPP life cycle needs to be studied,

including both the use phase and end-of-life phase, in order to incorporate recycling of metallic BPPs.

Regarding the environmental impact assessment, significant improvements could be achieved through the use of additional primary data. For this study, primary data was used only for furfural production and its upstream processes, sourced from a doctoral thesis based on data from an operational furfural production plant. Future work could enhance accuracy by obtaining data directly from the producer of furfural, Central Romana Corporation, thereby reducing the potential for misinterpretation.

This approach should also be applied to the graphite and bio-resin production processes. While acquiring primary data from a graphite producer in China may be challenging, Australian company Talga plans to begin graphite mining in Sweden, which may present an opportunity for primary data collection. Similarly, primary data for bio-resin production is available from the Belgian company TransFurans Chemicals (TFC), but due to time constraints, it was not utilized in this study. Incorporating this data in future work would enhance the robustness and accuracy of the environmental impact assessment.

9 Conclusion

This study has been conducted using a cradle-to-gate life cycle assessment approach to provide essential information regarding the environmental impacts of producing novel bio-based bipolar plates. In addition to the bio-based BPPs, two state-of-the-art materials were also included as comparisons.

The material comparison revealed that the bio-based BPP has the lowest overall environmental impact, while the metallic BPP has the highest, across almost all of the studied impact categories. This is primarily due to the lower emissions associated with the materials and energy sources used in the bio-based production system.

The results of the study indicate that the environmental impacts of producing the bio-based BPPs are spread across various impact categories. Furfural production in the Dominican Republic is the dominant contributor to most categories, particularly climate change, mainly due to its energy-intensive processes and reliance on a coal-based electricity grid. The findings also highlight that transportation of materials from distant sources such as graphite from China contributes significantly towards increased impact on climate change and acidification. Additionally, the core manufacturing process, compression moulding, contributes notably to several impact indicators due to its electricity consumption.

"A sensitivity analysis was conducted to assess how changes in the location of graphite mining would affect the results. Altering the graphite sourcing—by varying transport distances and electricity mixes, led to reductions across nearly all impact categories.

The performance assessment of the bio-based BPPs remains limited due to its early development stage. However, performance benchmarks have been obtained for future comparison of performances against the bio BPPs.

The primary limitation of this study is the lack of high-quality primary data for emerging bio-based technologies. To improve the reliability of future assessments, more detailed and process-specific data collection is needed. This would help refine the environmental profile of bio-based BPPs and enable more robust and comparable LCA results. Future research should also consider normalization and weighting to support clearer interpretation of environmental trade-offs.

10 Recommendation

To guide future research and improvements, the following recommendations are proposed for the BioBPP 2 project stakeholders and Volvo Group Trucks Technology, based on the findings of this study:

(a) Move towards composite BPPs with a higher content of renewable components.

(b) Produce graphite locally, if not possible in Sweden, then at least in Europe.

(c) Produce bio resin from locally available raw materials, to decrease transportation distances even further.

(d) Enhance data quality by conducting a life cycle assessment of bio-based bipolar plates using a greater proportion of primary data, particularly in the material production phase, to determine whether higher-quality data may influence the results.

(e) Perform a prospective LCA that explores the scalability of bio-based BPP production and incorporates future technological developments to assess the potential environmental impacts under future scenarios.

(f) Expand the system boundary to a cradle-to-grave LCA of the entire fuel cell system, integrating the current BPP LCA results, in order to understand the role and influence of bipolar plates on the overall environmental performance. Consideration of material recycling should also be included and evaluated.

(g) Conduct a comparative performance study across various materials, including additional metallic options, to enable more comprehensive and accurate material comparisons.

References

1. International Transport Forum (ITF). ITF Transport Outlook 2023. Tech. rep. Paris: OECD Publishing, 2023. DOI: 10.1787/b6cc9ad5-en. Available from: https://doi.org/10.1787/b6cc9ad5-en
2. Platform for Electromobility. Recommendations for the Deployment of Sustainable Infrastructure for BEHDVs. Accessed: 31-Jan-2025. 2023 Nov. Available from: https://www.platformelectromobility.eu/wp-content/uploads/2023/11/PfEM_Recommendations-for-the-deployment-of-sustainable-infrastructure-for-BEHDVs.pdf
3. Wang Y, Ruiz Diaz DF, Chen KS, Wang Z, and Adroher XC. Materials, technological status, and fundamentals of PEM fuel cells – A review. Materials Today 2020; 32:178–203. DOI: https://doi.org/10.1016/j.mattod.2019.06.005. Available from: https://www.sciencedirect.com/science/article/pii/S1369702119304948
4. Garbe JS. Life Cycle Assessment of PEM Fuel Cell Vehicles. Master's Thesis. Universitat Politècnica de Catalunya, 2020. Available from: https://upcommons.upc.edu/handle/2117/329732
5. BioInnovation. Renewable Bipolar Plates for Sustainable Fuel Cell Technology (BIOBPP 2 - Step 2). Accessed: 2025-06-23. 2025. Available from: https://www.bioinnovation.se/en/projekt/renewable-bipolar-plates-for-sustainable-fuel-cell-technology-biobpp-2-step-2/
6. Song Y, Zhang C, Ling CY, Han M, Yong RY, Sun D, and Chen J. Review on current research of materials, fabrication and application for bipolar plate in proton exchange membrane fuel cell. International Journal of Hydrogen Energy 2020; 45. Progress in Fuel Cells:29832–47. DOI: https://doi.org/10.1016/j.ijhydene.2019.07.231. Available from: https://www.sciencedirect.com/science/article/pii/S0360319919328745
7. Sharma P and Pandey O. Chapter 1 - Proton exchange membrane fuel cells: fundamentals, advanced technologies, and practical applications. *PEM Fuel Cells*. Ed. by Kaur G. Elsevier, 2022 :1–24. DOI: https://doi.org/10.1016/B978-0-12-823708-3.00006-7. Available from: https://www.sciencedirect.com/science/article/pii/B9780128237083000067
8. Group P. PowerCell P Stack. Accessed: February 11, 2025. 2024. Available from: https://25513287.fs1.hubspotusercontent-eu1.net/hubfs/25513287/PowerCell%20Group%20P%20Stack.pdf
9. Schumm B. Fuel Cell | Definition, Types, Applications, & Facts | Britannica. [Accessed: 18-Mar-2020]. 2020. Available from: https://www.britannica.com/technology/fuel-cell
10. Gao X, Chen J, Xu R, Zhen Z, Zeng X, Chen X, and Cui L. Research progress and prospect of the materials of bipolar plates for proton exchange membrane fuel cells (PEMFCs). International Journal of Hydrogen Energy 2024; 50:711–43. DOI: https://doi.org/10.1016/j.ijhydene.2023.09.005. Available from: https://www.sciencedirect.com/science/article/pii/S0360319923045688
11. Öztürk A, Akay RG, Erkan S, and Yurtcan AB. Chapter 1 - Introduction to fuel cells. *Direct Liquid Fuel Cells*. Ed. by Akay RG and Yurtcan AB. Academic Press, 2021 :1–47. DOI: https://doi.org/10.1016/B978-0-12-818624-4.00001-7. Available from: https://www.sciencedirect.com/science/article/pii/B9780128186244000017
12. Xu Z, Qiu D, Yi P, Peng L, and Lai X. Towards mass applications: A review on the challenges and developments in metallic bipolar plates for PEMFC. Progress in Natural Science: Materials International 2020; 30:815–24. DOI: https://doi.org/10.1016/j.pnsc.2020.10.015. Available from: https://www.sciencedirect.com/science/article/pii/S100200712030544X
13. Yi P, Zhang D, Qiu D, Peng L, and Lai X. Carbon-based coatings for metallic bipolar plates used in proton exchange membrane fuel cells. International Journal of Hydrogen Energy 2019; 44:6813–43. DOI: https://doi.org/10.1016/j.ijhydene.2019.01.176. Available from: https://www.sciencedirect.com/science/article/pii/S0360319919303350

14. Hauschild MZ, Rosenbaum RK, and Olsen SI, eds. Life Cycle Assessment: Theory and Practice. Cham, Switzerland: Springer International Publishing, 2018. DOI: 10.1007/978-3-319-56475-3. Available from: https://link.springer.com/book/10.1007/978-3-319-56475-3
15. Standardization IO for. ISO 14040:2006 – Environmental management – Life cycle assessment – Principles and framework. Geneva, 2006
16. Standardization IO for. ISO 14044:2006 – Environmental management – Life cycle assessment – Requirements and guidelines. Geneva, 2006
17. European Commission - Joint Research Centre (JRC). International Reference Life Cycle Data System (ILCD) Handbook. Luxembourg, 2010. Available from: https://eplca.jrc.ec.europa.eu/ilcd.html
18. Tillman HBAM, ed. The Hitch hiker's Guide to LCA – An orientation in life cycle assessment methodology and application, Lund, Sweden: Studentliteratur, 2004. Available from: https://www.studentlitteratur.se/kurslitteratur/naturvetenskap-och-miljo/miljo/the-hitch-hikers-guide-to-lca/
19. Ecoinvent. The Life Cycle Inventory Data Version 3.11. Accessed: 10-Feb-2025. 2024. Available from: https://support.ecoinvent.org/ecoinvent-version-3.11
20. Greendelta. openLCA v2.3.0. Accessed: 10-Feb-2025. 2025. Available from: https://www.openlca.org/
21. CML-IA. CML-IA Characterisation factors. Accessed: 20-Feb-2025. 2016. Available from: https://www.universiteitleiden.nl/en/%20research/research-output/science/cml-ia-characterisation-factors
22. Hauschild MZ, Rosenbaum RK, and Olsen SI, eds. Life Cycle Assessment: Theory and Practice. Cham, Switzerland: Springer International Publishing, 2018. DOI: 10.1007/978-3-319-56475-3. Available from: https://link.springer.com/book/10.1007/978-3-319-56475-3
23. Huijbregts M, Steinmann Z, Elshout P, Stam G, Verones F, Vieira M, Zijp M, Hollander A, and Zelm R. Correction to: ReCiPe2016: a harmonised life cycle impact assessment method at midpoint and endpoint level. The International Journal of Life Cycle Assessment 2020 Aug; 25:1–1. DOI: 10.1007/s11367-020-01761-5
24. Jabara M, Wu J, De Franceschi S, and Manzardo A. Assessing Mineral and Metal Resources in Life Cycle Assessment: An Overview of Existing Impact Assessment Methods. Sustainability 2025; 17. DOI: 10.3390/su17041692. Available from: https://www.mdpi.com/2071-1050/17/4/1692
25. Usai L, Hung CR, Vásquez F, Windsheimer M, Burheim OS, and Strømman AH. Life cycle assessment of fuel cell systems for light duty vehicles, current state-of-the-art and future impacts. Journal of Cleaner Production 2021; 280:125086. DOI: https://doi.org/10.1016/j.jclepro.2020.125086. Available from: https://www.sciencedirect.com/science/article/pii/S0959652620351301
26. Evangelisti S, Tagliaferri C, Brett DJ, and Lettieri P. Life cycle assessment of a polymer electrolyte membrane fuel cell system for passenger vehicles. Journal of Cleaner Production 2017; 142:4339–55. DOI: https://doi.org/10.1016/j.jclepro.2016.11.159. Available from: https://www.sciencedirect.com/science/article/pii/S0959652616320212
27. Simons A and Bauer C. A life-cycle perspective on automotive fuel cells. Applied Energy 2015; 157:884–96. DOI: https://doi.org/10.1016/j.apenergy.2015.02.049. Available from: https://www.sciencedirect.com/science/article/pii/S0306261915002263
28. Atlas Steels. Stainless Steel Grade Datasheets. https://kh.aquaenergyexpo.com/wp-content/uploads/2023/02/Stainless-Steel-Grade-Datasheets.pdf. Accessed: May 30, 2025. 2023
29. Stainless Steel Co., Ltd. 304 Stainless Steel Sheet. https://stainlesteel.cn/portfolio-item/304-stainless-steel-sheet. Accessed: May 30, 2025. 2023

30. Stainless Steel Co., Ltd. 316 Stainless Steel Sheet. https://stainlesteel.cn/portfolio-item/316-stnless-steel-sheet. Accessed: May 30, 2025. 2023
31. Lentatek. Proton Exchange Membrane Fuel Cell (PEMFC) Bipolar Plate (BPP). Accessed: 2025-05-23. 2025. Available from: https://www.lentatek.com/en/solutions/hydrogen-and-fuel-cell-technologies/proton-exchange-membrane-fuel-cell-pemfc-bipolar-plate-bpp
32. Gong G. Personal communication regarding the BioBPP 2 project. Project manager, RISE Research Institutes of Sweden, communicated May 2025. 2025
33. Haase S, Moser M, Hirschfeld J, and Jozwiak K. Current density and catalyst-coated membrane resistance distribution of hydro-formed metallic bipolar plate fuel cell short stack with 250 cm2 active area. Journal of Power Sources 2016; 301:251–60. DOI: https://doi.org/10.1016/j.jpowsour.2015.09.118. Available from: https://www.sciencedirect.com/science/article/pii/S0378775315303852
34. Iranzo A, Toharias B, Suárez C, Rosa F, and Pino J. Dataset and mesh of the CFD numerical model for the modelling and simulation of a PEM fuel cell. Data in Brief 2022; 41:107987. DOI: https://doi.org/10.1016/j.dib.2022.107987. Available from: https://www.sciencedirect.com/science/article/pii/S2352340922001986
35. Survey UG. Mineral Commodity Summaries. Accessed: 2025-04-05. 2024. Available from: https://pubs.usgs.gov/periodicals/mcs2024/mcs2024-graphite.pdf?utm_source=2and20.beehiiv.com&utm_medium=referral&utm_campaign=disaster-in-the-oval-office
36. TransFurans Chemicals. Sustainability. https://www.transfurans.be/sustainability. Accessed: May 30, 2025. 2023
37. Blanco J. Environmental and economic assessment and optimization of a novel technology for furfural production through life cycle tools. 2024. Accessed: 2025-03-13. Available from: https://www.mdpi.com/2071-1050/17/4/1692
38. Garg S. Europe Phenolic Resin Market Outlook to 2028. Accessed: 2025-04-05. 2024. Available from: https://www.kenresearch.com/industry-reports/europe-phenolic-resin-market
39. Khanal A, Manandhar A, Adhikari S, and Shah A. Techno-economic analysis of novolac resin production by partial substitution of petroleum-derived phenol with bio-oil phenol. Biofuels, Bioproducts and Biorefining 2021 Jul; 15. DOI: 10.1002/bbb.2268
40. Bi J, Yang J, Liu X, Wang D, Yang Z, Liu G, and Wang X. Development and evaluation of nitride coated titanium bipolar plates for PEM fuel cells. International Journal of Hydrogen Energy 2021; 46:1144–54. DOI: https://doi.org/10.1016/j.ijhydene.2020.09.217. Available from: https://www.sciencedirect.com/science/article/pii/S0360319920336879
41. Reck B, Chambon M, Hashimoto S, and Graedel T. Global Stainless Steel Cycle Exemplifies China's Rise to Metal Dominance. Environmental science technology 2010 May; 44:3940–6. DOI: 10.1021/es903584q
42. Gabriel Fraga Jerome Ramirez MR. Conceptual Process Design, Techno-economics, and Greenhouse Gas Analysis of Furfuryl Alcohol via Transfer Hydrogenation. ACS Sustainable Chem 2024; 12. Accessed: 2025-03-14. Available from: https://doi.org/10.1021/acssuschemeng.4c03588
43. Elsa Weiszflog MA. Life Cycle Assessment of Hydrogen Storage Systems for Trucks. 2022. Accessed: 2025-02-14. Available from: https://odr.chalmers.se/server/api/core/bitstreams/2a16256f-2858-4f55-972f-a6889d05e252/content
44. Irshad HM and Shahgaldi S. Comprehensive review of bipolar plates for proton exchange membrane fuel cells with a focus on materials, processing methods and characteristics. International Journal of Hydrogen Energy 2025; 111:462–87. DOI: https://doi.org/10.1016/j.ijhydene.2025.02.300. Available from: https://www.sciencedirect.com/science/article/pii/S036031992500878X

45. Tang A, Crisci L, Bonville L, and Jankovic J. An overview of bipolar plates in proton exchange membrane fuel cells. Journal of Renewable and Sustainable Energy 2021; 13:022701. DOI: 10.1063/5.0031447. Available from: https://doi.org/10.1063/5.0031447
46. HYCCO. Composite Bipolar Plates Datasheet for the Next Generation of Fuel Cells and Redox Flow Batteries. Accessed: 2025-05-23. 2022. Available from: https://hycco.fr/wp-content/uploads/2022/07/Data-sheet-V11low.pdf
47. Chaiwan P, Sarakonsri T, and Pumchusak J. Electrical and Mechanical Properties of Surface Functionalized Carbon Nanotubes Incorporated Graphite-Phenolic Composite Bipolar Plate for PEMFC. *Proceeding of International Conference on Mining, Material and Metallurgical Engineering 2016*. Vol. 707. Key Engineering Materials. Trans Tech Publications Ltd, 2016 Oct :23–7. DOI: 10.4028/www.scientific.net/KEM.707.23
48. Xu G, Du X, Chang L, Hu X, and Song J. Effect of molding temperature on the properties of phenolic resin/carbon black/graphite composite bipolar plates. Journal of Solid State Electrochemistry 2024; 28:2505–13. DOI: 10.1007/s10008-023-05798-y
49. Song Y, Zhang C, Ling CY, Han M, Yong RY, Sun D, and Chen J. Review on current research of materials, fabrication and application for bipolar plate in proton exchange membrane fuel cell. International Journal of Hydrogen Energy 2020; 45. Progress in Fuel Cells:29832–47. DOI: https://doi.org/10.1016/j.ijhydene.2019.07.231. Available from: https://www.sciencedirect.com/science/article/pii/S0360319919328745
50. Huang P, Chen Z, Zhang J, Wu M, Liu Y, Zhang F, Chen Y, and Chen X. Stainless steel bipolar plate fuel cell with different flow field structures prepared by laser additive manufacturing. International Journal of Heat and Mass Transfer 2022; 183:122186. DOI: https://doi.org/10.1016/j.ijheatmasstransfer.2021.122186. Available from: https://www.sciencedirect.com/science/article/pii/S0017931021012850
51. Gao X, Chen J, Xu R, Zhen Z, Zeng X, Chen X, and Cui L. Research progress and prospect of the materials of bipolar plates for proton exchange membrane fuel cells (PEMFCs). International Journal of Hydrogen Energy 2024; 50:711–43. DOI: https://doi.org/10.1016/j.ijhydene.2023.09.005. Available from: https://www.sciencedirect.com/science/article/pii/S0360319923045688
52. Name A. Title of the Article. Polymer Advanced Technology Year of Publication; Volume Number:Page Range. DOI: 10.1002/pat.6301
53. Jeong KI, Oh J, Song SA, Lee D, Lee DG, and Kim SS. A review of composite bipolar plates in proton exchange membrane fuel cells: Electrical properties and gas permeability. Composite Structures 2021; 262:113617. DOI: https://doi.org/10.1016/j.compstruct.2021.113617. Available from: https://www.sciencedirect.com/science/article/pii/S0263822321000787
54. Jannat S, Rashtchi H, Atapour M, Golozar MA, Elmkhah H, and Zhiani M. Preparation and performance of nanometric Ti/TiN multi-layer physical vapor deposited coating on 316L stainless steel as bipolar plate for proton exchange membrane fuel cells. Journal of Power Sources 2019; 435:226818. DOI: https://doi.org/10.1016/j.jpowsour.2019.226818. Available from: https://www.sciencedirect.com/science/article/pii/S0378775319308092
55. Choi JH, Eun Kang H, Kim DJ, and Soo Yoon Y. A Comprehensive Review of Stainless-Steel Bipolar Plate Coatings and Their Role in Mitigating Corrosion in Aggressive Proton-Exchange Membrane Fuel Cells Environments. Chemical Engineering Journal 2024; 493:152662. DOI: https://doi.org/10.1016/j.cej.2024.152662. Available from: https://www.sciencedirect.com/science/article/pii/S1385894724041494
56. Ma S. Progress in the study of bipolar plates/conductive fillers. Advances in Engineering Technology Research 2023; 8:581–92. DOI: 10.56028/aetr.8.1.581.2023. Available from: https://doi.org/10.56028/aetr.8.1.581.2023
57. LyondellBasell. BMC 940 8649 Technical Data Sheet. Accessed: 2025-05-23. 2020. Available from: https://www.lyondellbasell.com/globalassets/products-technology/

advanced-polymer-solutions/technical-data-sheets/bulk-molding-compounds/bmc.940.8649.tds_1.16.2020.pdf

58. Tang W, Wang S, Li S, Yu S, Yuan X, Yang C, and Li W. Research progress on coating and coating technology of fuel cell metallic bipolar plate. Next Materials 2024; 4:100062. DOI: https://doi.org/10.1016/j.nxmate.2023.100062. Available from: https://www.sciencedirect.com/science/article/pii/S294982282300062X
59. Xu G, Du X, Chang L, Hu X, and Song J. Effect of molding temperature on the properties of phenolic resin/carbon black/graphite composite bipolar plates. Journal of Solid State Electrochemistry 2024; 28:2505–13. DOI: 10.1007/s10008-023-05798-y. Available from: https://doi.org/10.1007/s10008-023-05798-y
60. Kuan YD, Ciou CW, Shen MY, Wang CK, Fitriani RZ, and Lee CY. Bipolar plate design and fabrication using graphite reinforced composite laminate for proton exchange membrane fuel cells. International Journal of Hydrogen Energy 2021; 46. SEGT-2019:16801–14. DOI: https://doi.org/10.1016/j.ijhydene.2020.08.030. Available from: https://www.sciencedirect.com/science/article/pii/S0360319920330251

Appendix A - Calculations

SotA Composite BPP

All relevant data for this calculation, is shown in Table 16. The first step involves calculating the total front area of the bipolar plate. This is done by multiplying the active area with the average fraction between the total area and the active area, as shown in eq. (1).

Table 16: SotA composite calculation data

Parameter	Description	Value	Unit
A_{active}	Active area	800	cm^2
t	thickness	0.2	cm
L	Volume losses	33	%
ρ	Density	2	g/cm^3
n_{cell}	Number of cells	157	
P_{stack}	Power output of the stack	120	kW

The total area is then approximated to 1695.6 cm^2. By multiplying the total area with thickness, the total volume of the BPP is obtained as seen by eq. (2). This gives the total volume of the BPP of 339.12 cm^3. However, approximetly 33% of volume is lost in the channels on the BPP, hence the true volume of the plate is 227.21 cm^3 as seen in eq. (3). The weight per plate is calculated through eq. (4) and is equal to 454.4 g/BPP. The number of bipolar plates in a FC stack is shown in eq. (5), which in this case is 158. The total weight of BPP is calculated with eq. (6), which is 71.79 kg. The weight per power output is lastly calculated with eq. (7) which equates to 0.598 kg/kW for the state-of-the-art composite BPP.

$$A_{tot} = A_{active} \cdot 2.12 \tag{1}$$

$$V_{tot} = A_{tot} \cdot t \tag{2}$$

$$V_{real} = V_{tot} \cdot (1 - 0.33) \tag{3}$$

$$m_{BPP} = V_{real} \cdot \rho \tag{4}$$

$$n_{BPP} = n_{cell} + 1 \tag{5}$$

$$m_{tot} = n_{BPP} \cdot m_{BPP} \tag{6}$$

$$m/P = m_{tot}/P_{stack} \tag{7}$$

Metallic BPP

All relevant data for this calculation is shown in Table 17. The first step involves calculating the total front area of the bipolar plate. This is done by multiplying the active area with the average fraction between the total area and the active area, as shown in eq. (1).

Table 17: Metallic BPP calculation data

Parameter	Description	Value	Unit
A_{active}	Active area	800	cm^2
t	thickness	0.02	cm
ρ	Density	8.2	g/cm^3
n_{cell}	Number of cells	146	
P_{stack}	Power output of the stack	120	kW

The total area is then approximated to 1695.6 cm^2. By multiplying the total area with thickness, the total volume of the BPP is obtained as seen by eq. (2). This gives the total volume of the BPP of 33.91 cm^3. For the metallic BPP, there is no volume losses. The weight per plate is calculated through eq. (4) and is equal to 278.1.4 g/BPP. The number of bipolar plates in a FC stack is shown in eq. (5), which in this case is 147. The total weight of BPP is calculated with eq. (6), which is 40.88 kg. The weight per power output is lastly calculated with eq. (7) which equates to 0.341 kg/kW for the metallic.

The second part of the calculation involves calculating the surface area which will undergo coating. One side of the BPP has a total surface area of 1695.6 cm^2. As one BPP is made up of two halves, the total number of surfaces needed to be coated is four, which results in the total surface area per BPP equal 6782.4 cm^2. Now the total coating area is calculated with eq. (8), which equals 99.7 m^2. The coating area per kW is obtained through eq. (9), which results in 0.831 m^2/kW.

$$A_{coat,tot} = n_{BPP} \cdot A_{coat,BPP} \tag{8}$$

$$A/P = A_{coat,tot}/P_{stack} \tag{9}$$

Bio BPP

All relevant data for this calculation is shown in Table 18. This calculation is done in two simple steps, by obtaining the power output of the cell through eq. (10). Then the weight of the cell is divided by the power output, as seen in eq. (11). This results in a weight to power ratio of 0.433 kg/kW.

Table 18: Bio-based BPP calculation data

Parameter	Description	Value	Unit
m_{BPP}	weight of 1 BPP	70	g
V_{cell}	Cell voltage	1.1	V
I_{cell}	Cell current	147	A

$$P_{cell} = V_{cell} \cdot I_{cell} \tag{10}$$

$$m/P = m_{cell}/P_{cell} \tag{11}$$

Appendix B - Inventory data

Inventory Data – Bio based BPP System

Bio-based BPP Production - After testing (Power Based)			
Input			
Flow	Amount	Unit	Provider
Bio-based BPP (After compression moulding)	0.832	kg	Bio based material -Compression Moulding -New
Output			
Flow	Amount	Unit	
Bio-based BPP (After testing-Power based)	1.0	kW	
Bio based material -Compression Moulding			
Input			
Flow	Amount	Unit	Provider
Bio carbon transported	0.1	kg	Transportation of Bio carbon
Bio-resin transported	0.2	kg	Transportation of Bio-resin
electricity, low voltage	1.5	kWh	market for electricity, low voltage | electricity, low voltage | Cutoff, U - SE
heat, district or industrial, natural gas	4.84	MJ	market for heat, district or industrial, natural gas | heat, district or industrial, natural gas | Cutoff, U - Europe without Switzerland
light fuel oil	3.9E-4	kg	market for light fuel oil | light fuel oil | Cutoff, U - Europe without Switzerland
lubricating oil	8.39E-4	kg	market for lubricating oil | lubricating oil | Cutoff, U - RER
Natural flake graphite transported	0.7	kg	Transportation of Natural flake graphite
Output			
Bio-based BPP (After compression moulding)	1.0	kg	

Transportation of Bio carbon			
Input			
Flow	Amount	Unit	Provider
Biocarbon pellet	1.0	kg	Biocarbon pellet production | wood pellet, measured as dry mass | Cutoff, U (copy) - RER
transport, freight, lorry, 3.5-7.5 metric ton, diesel, EURO 6	1.0	t*km	
Output			
Bio carbon transported	1.0	kg	
Transportation of Bio-resin			
Input			
Flow	Amount	Unit	Provider
Bio-resin	1.0	kg	Production of Bio-resin
transport, freight, lorry, >32 metric ton, diesel, EURO 6	1*1600	kg*km	transport, freight, lorry, >32 metric ton, diesel, EURO 6 | transport, freight, lorry, >32 metric ton, diesel, EURO 6 | Cutoff, U - RER
Output			
Bio-resin transported	1.0	kg	
Transportation of Natural flake graphite			
Input			
Flow	Amount	Unit	Provider
graphite	1.0	kg	graphite production | graphite | Cutoff, U (modified) - CN

transport, freight, lorry, >32 metric ton, diesel, EURO 6	1.0*1000	kg*km	transport, freight, lorry, >32 metric ton, diesel, EURO 6 | transport, freight, lorry, >32 metric ton, diesel, EURO 6 | Cutoff, U - RER
transport, freight, sea, bulk carrier for dry goods, heavy fuel oil	1.0*17500	kg*km	transport, freight, sea, bulk carrier for dry goods, heavy fuel oil | transport, freight, sea, bulk carrier for dry goods, heavy fuel oil | Cutoff, U - GLO
Output			
Natural flake graphite transported	1.0	kg	
Production of Bioresin			
Input			
Flow	Amount	Unit	Provider
heat, from steam, in chemical industry	0.399063145089249	kWh	market for heat, from steam, in chemical industry | heat, from steam, in chemical industry | Cutoff, U - RER
Furfuryl Alcohol (FA)	1.052	kg	Production of Furfuryl Alcohol
Output			
Bio-resin	1.0	kg	

Biocarbon pellet production | wood pellet, measured as dry mass | Cutoff, U (modified)			
Input			
Flow	Amount	Unit	Provider
Biochar	0.095	kg	Biochar Pyrolysis
dust collector, electrostatic precipitator, for industrial use	1.0E-9	Item(s)	market for dust collector, electrostatic precipitator, for industrial use | dust collector, electrostatic precipitator, for industrial use | Cutoff, U - GLO
dust collector, multicyclone	1.0E-9	Item(s)	market for dust collector, multicyclone | dust collector, multicyclone | Cutoff, U - GLO

electricity, medium voltage	0.096	kWh	market for electricity, medium voltage | electricity, medium voltage | Cutoff, U - SE
heat, central or small-scale, other than natural gas	3.45	MJ	heat production, at heat pump 30kW, allocation exergy | heat, central or small-scale, other than natural gas | Cutoff, U - Europe without Switzerland
lubricating oil	8.4E-5	kg	market for lubricating oil | lubricating oil | Cutoff, U - RER
maize starch	0.005	kg	market for maize starch | maize starch | Cutoff, U - GLO
wood pellet factory	4.0E-10	Item(s)	wood pellet factory production | wood pellet factory | Cutoff, U - RER
Water, unspecified natural origin	3.0E-5	m3	
Output			
Biocarbon pellet	1.0	kg	
waste mineral oil	2.224617980688103E-6	kg	market for waste mineral oil | waste mineral oil | Cutoff, U - CH
waste mineral oil	8.177538201931189E-5	kg	market for waste mineral oil | waste mineral oil | Cutoff, U - Europe without Switzerland
Water	4.5E-6	m3	
Water	2.55E-5	m3	
Biochar Pyrolysis			
Input			
Flow	Amount	Unit	Provider
electricity, medium voltage	2.5	MJ	market for electricity, medium voltage | electricity, medium voltage | Cutoff, U - SE
wood chips, dry, measured as dry mass	1.98	kg	market for wood chips, dry, measured as dry mass | wood chips, dry, measured as dry mass | Cutoff, U - RER
Output			
Biochar	1.0	kg	
Production of Furfuryl Alcohol			

Input			
Flow	Amount	Unit	Provider
electricity, medium voltage	0.02	kWh	market for electricity, medium voltage | electricity, medium voltage | Cutoff, U - BE
Furfural (sugarcane residue product) transported	1.055	kg	Transportation of Furfural (sugarcane residue product)
hydrogen, gaseous, low pressure	0.024	kg	hydrogen production, steam methane reforming | hydrogen, gaseous, low pressure | Cutoff, U - RER
steam, in chemical industry	9.8E-5	t	steam production, in chemical industry | steam, in chemical industry | Cutoff, U - RER
Output			
Furfuryl Alcohol (FA)	1.0	kg	
spent solvent mixture	0.061	kg	treatment of spent solvent mixture, hazardous waste incineration | spent solvent mixture | Cutoff, U - Europe without Switzerland
Transportation of Furfural (sugarcane residue product)			
Input			
Flow	Amount	Unit	Provider
Furfural	1.0	kg	Production of Furfural - DO
transport, freight, lorry, >32 metric ton, diesel, EURO 6	1.0*500	kg*km	transport, freight, lorry, >32 metric ton, diesel, EURO 6 | transport, freight, lorry, >32 metric ton, diesel, EURO 6 | Cutoff, U - RER

transport, freight, sea, tanker for liquid goods other than petroleum and liquefied natural gas, heavy fuel oil	1.0*8000	kg*km	transport, freight, sea, tanker for liquid goods other than petroleum and liquefied natural gas, heavy fuel oil | transport, freight, sea, tanker for liquid goods other than petroleum and liquefied natural gas, heavy fuel oil | Cutoff, U - GLO
Output			
Furfural (sugarcane residue product) transported	1.0	kg	
Production of Furfural			
Input			
Flow	Amount	Unit	Provider
bagasse, from sugarcane	6.7	kg	sugarcane processing, traditional annexed plant | bagasse, from sugarcane | Cutoff, U - RoW
electricity, low voltage	0.030364	kWh	market for electricity, low voltage | electricity, low voltage | Cutoff, U - DO
soda ash, dense	0.006	kg	market for soda ash, dense | soda ash, dense | Cutoff, U - GLO
steam, in chemical industry	0.4	kg	steam production, in chemical industry | steam, in chemical industry | Cutoff, U - RoW
steam, in chemical industry	0.33	kg	steam production, in chemical industry | steam, in chemical industry | Cutoff, U - RoW
sulfuric acid	0.15	kg	market for sulfuric acid | sulfuric acid | Cutoff, U - RoW
water, completely softened	1.8	kg	water production, completely softened | water, completely softened | Cutoff, U - RoW
Water, cooling, unspecified natural origin	291.95	m3	
Output			
Furfural	1.0	kg	

Solid biomass waste	4.6	kg	
Carbon dioxide, fossil	0.001	kg	
Water	20.4	m3	
Market for Electricity- SE			
Input	Amount	Unit	Provider
electricity, medium voltage	0.00403007424286678	kWh	market for electricity, medium voltage | electricity, medium voltage | Cutoff, U - SE
electricity, medium voltage	0.0272530677179305	kWh	electricity, from municipal waste incineration to generic market for electricity, medium voltage | electricity, medium voltage | Cutoff, U - SE
electricity, medium voltage	0.97274693228207	kWh	electricity voltage transformation from high to medium voltage | electricity, medium voltage | Cutoff, U - SE
sulfur hexafluoride, liquid	1.13E-7	kg	market for sulfur hexafluoride, liquid | sulfur hexafluoride, liquid | Cutoff, U - RER
transmission network, electricity, medium voltage	1.86277676887616E-8	km	market for transmission network, electricity, medium voltage | transmission network, electricity, medium voltage | Cutoff, U - GLO

Inventory Data – SotA Composite System

Production SotA Composite BPP - After Testing			
Input			
Flow	Amount	Unit	Provider
SotA Composite BPP (After Compression Moulding)	0.832	kg	SotA Composite BPP -Compression Moulding
Output			
Flow	Amount	Unit	
SotA Composite BPP (After testing-Power Based)	1.0	kW	

Production SotA Composite BPP -Compression Moulding			
Input			
Flow	Amount	Unit	Provider
electricity, low voltage	1.5	kWh	market for electricity, low voltage | electricity, low voltage | Cutoff, U - SE
heat, district or industrial, natural gas	4.84	MJ	market for heat, district or industrial, natural gas | heat, district or industrial, natural gas | Cutoff, U - Europe without Switzerland
light fuel oil	3.9E-4	kg	market for light fuel oil | light fuel oil | Cutoff, U - Europe without Switzerland
lubricating oil	8.39E-4	kg	market for lubricating oil | lubricating oil | Cutoff, U - RER
Natural flake graphite transported	0.8	kg	Transportation of Natural flake graphite
Phenolic resin transported	0.2	kg	Transportation of Phenolic Resin
Output			
SotA Composite BPP (After Compression Moulding)	1.0	kg	
bilge oil	0.001229	kg	market for bilge oil | bilge oil | Cutoff, U - Europe without Switzerland

Transportation of Natural flake graphite

Input			
graphite	1.0	kg	graphite production | graphite | Cutoff, U (copy) - CN
transport, freight, lorry, >32 metric ton, diesel, EURO 6	1.0*1000	kg*km	transport, freight, lorry, >32 metric ton, diesel, EURO 6 | transport, freight, lorry, >32 metric ton, diesel, EURO 6 | Cutoff, U - RER
transport, freight, sea, bulk carrier for dry goods, heavy fuel oil	1.0*17500	kg*km	transport, freight, sea, bulk carrier for dry goods, heavy fuel oil | transport, freight, sea, bulk carrier for dry goods, heavy fuel oil | Cutoff, U - GLO
Output			
Natural flake graphite transported	1.0	kg	

Transportation of Phenolic Resin			
Input			
phenolic resin	1.0	kg	phenolic resin production | phenolic resin | Cutoff, U - RER
transport, freight, lorry, 16-32 metric ton, diesel, EURO 6	1.0*1500	kg*km	transport, freight, lorry, 16-32 metric ton, diesel, EURO 6 | transport, freight, lorry, 16-32 metric ton, diesel, EURO 6 | Cutoff, U - RER
Output			
Phenolic resin transported	1.0	kg	

graphite production | graphite | Cutoff, U (modified)			
Input			
Flow	Amount	Unit	Provider
blasting	7.73E-5	kg	market for blasting | blasting | Cutoff, U - GLO
conveyor belt	2.78E-8	m	market for conveyor belt | conveyor belt | Cutoff, U - GLO
diesel, burned in building machine	0.018	MJ	market for diesel, burned in building machine | diesel, burned in building machine | Cutoff, U - GLO
electricity, medium voltage	0.0022625930897302885	kWh	market group for electricity, medium voltage | electricity, medium voltage | Cutoff, U - CN
electricity, medium voltage	3.071351784915626E-4	kWh	market group for electricity, medium voltage | electricity, medium voltage | Cutoff, U - CN
electricity, medium voltage	0.007150361538118727	kWh	market group for electricity, medium voltage | electricity, medium voltage | Cutoff, U - CN
electricity, medium voltage	0.021597245765567954	kWh	market group for electricity, medium voltage | electricity, medium voltage | Cutoff, U - CN
electricity, medium voltage	6.402281438392787E-5	kWh	market group for electricity, medium voltage | electricity, medium voltage | Cutoff, U - CN
electricity, medium voltage	0.001103999857448205 8	kWh	market group for electricity, medium voltage | electricity, medium voltage | Cutoff, U - CN
electricity, medium voltage	1.4641756259345751E-5	kWh	market group for electricity, medium voltage | electricity, medium voltage | Cutoff, U - CN
heat, central or small-scale, other than natural gas	0.0033746	MJ	market for heat, central or small-scale, other than natural gas | heat, central or small-scale, other than natural gas | Cutoff, U - RoW
heat, district or industrial, other than natural gas	0.0897584165864674	MJ	market for heat, district or industrial, other than natural gas | heat, district or industrial, other than natural gas | Cutoff, U - RoW
heat, district or industrial, other than natural gas	4.1583413532607136E-5	MJ	market for heat, district or industrial, other than natural gas | heat, district or industrial, other than natural gas | Cutoff, U - RoW
industrial machine, heavy, unspecified	2.31E-4	kg	market for industrial machine, heavy, unspecified | industrial machine, heavy, unspecified | Cutoff, U - RoW
limestone quarry infrastructure	5.25E-11	Item(s)	market for limestone quarry infrastructure | limestone quarry infrastructure | Cutoff, U - GLO
recultivation, limestone mine	6.52E-6	m2	market for recultivation, limestone mine | recultivation, limestone mine | Cutoff, U - GLO
Graphite	1.0526	kg	
Occupation, mineral extraction site	8.48E-5	m2*a	

Transformation, from forest, unspecified	6.52E-6	m2	
Transformation, to mineral extraction site	6.52E-6	m2	
Water, well, in ground	2.93E-5	m3	
Output			
graphite	1.0	kg	
Particulate Matter, < 2.5 um	8.87E-6	kg	
Particulate Matter, > 10 um	1.21E-4	kg	
Particulate Matter, > 2.5 um and < 10um	4.78E-5	kg	
Water	1.465E-5	m3	
Water	1.465E-5	m3	

phenolic resin production | phenolic resin | Cutoff, U			
Input			
Flow	Amount	Unit	Provider
chemical factory, organics	4.0E-10	Item(s)	chemical factory construction, organics | chemical factory, organics | Cutoff, U - RER
electricity, medium voltage	0.399063145089249	kWh	market group for electricity, medium voltage | electricity, medium voltage | Cutoff, U - RER
formaldehyde	0.152	kg	market for formaldehyde | formaldehyde | Cutoff, U - RER
phenol	0.95	kg	market for phenol | phenol | Cutoff, U - RER
Water, cooling, unspecified natural origin	0.0147069911293363	m3	
Water, river	9.65426270193802E-4	m3	
Water, well, in ground	8.16521839372613E-4	m3	
Output			
phenolic resin	1.0	kg	
wastewater, average	2.2212955346956164E-6	m3	market for wastewater, average | wastewater, average | Cutoff, U - Europe without Switzerland
wastewater, average	5.582444451470342E-8	m3	market for wastewater, average | wastewater, average | Cutoff, U - CH
BOD5, Biological Oxygen Demand	0.00418650658418539	kg	

Carbon dioxide, fossil	0.0468	kg	
COD, Chemical Oxygen Demand	0.00418650658418539	kg	
DOC, Dissolved Organic Carbon	0.00141731846160123	kg	
Formaldehyde	3.03E-4	kg	
Formaldehyde	2.73E-4	kg	
Phenol	0.0019	kg	
Phenol	0.00171	kg	
TOC, Total Organic Carbon	0.00141731846160123	kg	
Water	0.00147007593106921	m3	
Water	0.0150390618655492	m3	

Inventory Data – Metallic BPP System

Production of Metallic BPP - After Testing (Power based)			
Input			
Flow	Amount	Unit	Provider
Metallic BPP Product -After Coating	0.1585	kg	Production of Metallic BPP -After Coating
Output			
Flow	Amount	Unit	
Metallic BPP-After Testing	1.0	kW	

Production of Metallic BPP - After Coating (mass based)			
Input			
Flow	Amount	Unit	Provider
selective coat, copper sheet, physical vapour deposition	0.16	m2	selective coating, copper sheet, physical vapour deposition | selective coat, copper sheet, physical vapour deposition | Cutoff, U - DE
Stamped Stainless Steel - Metallic BPP	0.1585	kg	Stainless Steel Stamping - Metallic BPP
Output			
Metallic BPP Product -After Coating	0.1585	kg	

Stainless Steel Stamping			
Input			
Flow	Amount	Unit	Provider
deep drawing, steel, 650 kN press, single stroke	0.1585	kg	deep drawing, steel, 650 kN press, single stroke | deep drawing, steel, 650 kN press, single stroke | Cutoff, U (copy) - RER
Stainless steel 316 transported	0.1585	kg	Transportation of stainless steel
Output			
Stamped Stainless Steel - Metallic BPP	0.1585	kg	

selective coating, copper sheet, physical vapour deposition | selective coat, copper sheet, physical vapour deposition | Cutoff, U - DE			
Input			
Flow	Amount	Unit	Provider
electricity, medium voltage	1.2	kWh	market for electricity, medium voltage | electricity, medium voltage | Cutoff, U - DE
lubricating oil	1.68E-5	kg	market for lubricating oil | lubricating oil | Cutoff, U - RER
metal coating facility	3.33E-7	Item(s)	metal coating facility construction | metal coating facility | Cutoff, U - RER
nitrogen, liquid	0.00182	kg	market for nitrogen, liquid | nitrogen, liquid | Cutoff, U - RER
oxygen, liquid	9.09E-4	kg	market for oxygen, liquid | oxygen, liquid | Cutoff, U - RER
silica sand	8.9E-4	kg	market for silica sand | silica sand | Cutoff, U - GLO
titanium dioxide	0.001	kg	market for titanium dioxide | titanium dioxide | Cutoff, U - RER
Water, unspecified natural origin	0.007236	m3	
Output			
selective coat, copper sheet, physical vapour deposition	1.0	m2	
Water	0.0010854	m3	
Water	0.0061506	m3	

Transportation of Stainless Steel 316 to Metallic BPP Production Site			
Input			
Flow	Amount	Unit	Provider
steel, chromium steel 18/8, hot rolled	1.0	kg	market for steel, chromium steel 18/8, hot rolled | steel, chromium steel 18/8, hot rolled | Cutoff, U (modified) - GLO

transport, freight, sea, container ship, heavy fuel oil	1*17500	kg*km	market for transport, freight, sea, container ship, heavy fuel oil | transport, freight, sea, container ship, heavy fuel oil | Cutoff, U - GLO
Output			
Stainless steel 316 transported	1.0	kg	

deep drawing, steel, 650 kN press, single stroke | deep drawing, steel, 650 kN press, single stroke | Cutoff, U (copy)			
Input			
Flow	Amount	Unit	Provider
compressed air, 700 kPa gauge	4.45E-4	m3	market for compressed air, 700 kPa gauge | compressed air, 700 kPa gauge | Cutoff, U - RER
electricity, low voltage	0.0333	kWh	market group for electricity, low voltage | electricity, low voltage | Cutoff, U - RER
energy and auxilliary inputs, metal working factory	1.0	kg	market for energy and auxilliary inputs, metal working factory | energy and auxilliary inputs, metal working factory | Cutoff, U - RER
metal working factory	4.58E-10	Item(s)	metal working factory construction | metal working factory | Cutoff, U - RER
metal working machine, unspecified	7.79E-5	kg	market for metal working machine, unspecified | metal working machine, unspecified | Cutoff, U - RER
Output			
deep drawing, steel, 650 kN press, single stroke	1.0	kg	

market for steel, chromium steel 18/8 | steel, chromium steel 18/8 | Cutoff, U (modified) - GLO			
Input			
Flow	Amount	Unit	Provider
steel, chromium steel 18/8	0.130319047071891	kg	steel production, electric, chromium steel 18/8 | steel, chromium steel 18/8 | Cutoff, U (copy) - RER
steel, chromium steel 18/8	0.869680952928109	kg	steel production, electric, chromium steel 18/8 | steel, chromium steel 18/8 | Cutoff, U (copy) - RoW

transport, freight, inland waterways, barge, diesel	0.0201	t*km	market group for transport, freight, inland waterways, barge, diesel | transport, freight, inland waterways, barge, diesel | Cutoff, U - GLO
transport, freight, lorry, diesel, unspecified	0.2065	t*km	market group for transport, freight, lorry, diesel, unspecified | transport, freight, lorry, diesel, unspecified | Cutoff, U - GLO
transport, freight, sea, bulk carrier for dry goods, heavy fuel oil	0.4409	t*km	market for transport, freight, sea, bulk carrier for dry goods, heavy fuel oil | transport, freight, sea, bulk carrier for dry goods, heavy fuel oil | Cutoff, U - GLO
transport, freight, train, fleet average	0.1903	t*km	market group for transport, freight, train, fleet average | transport, freight, train, fleet average | Cutoff, U - GLO
Output			
steel, chromium steel 18/8	1.0	kg	

steel production, electric, chromium steel 18/8 | steel, chromium steel 18/8 | Cutoff, U (modified)			
Input			
Flow	Amount	Unit	Provider
anode, for metal electrolysis	0.004	kg	market for anode, for metal electrolysis | anode, for metal electrolysis | Cutoff, U - GLO
argon, liquid	0.032	kg	market for argon, liquid | argon, liquid | Cutoff, U - RER
electric arc furnace	4.0E-11	Item(s)	market for electric arc furnace | electric arc furnace | Cutoff, U - GLO
electricity, medium voltage	0.625	kWh	market group for electricity, medium voltage | electricity, medium voltage | Cutoff, U - RER
ferrochromium, high-carbon, 68% Cr	0.26471	kg	market for ferrochromium, high-carbon, 68% Cr | ferrochromium, high-carbon, 68% Cr | Cutoff, U - GLO
ferronickel	0.44	kg	market for ferronickel | ferronickel | Cutoff, U - GLO
hard coal	0.0091651513891168	kg	market group for hard coal | hard coal | Cutoff, U - RER
iron scrap, sorted, pressed	0.407	kg	market for iron scrap, sorted, pressed | iron scrap, sorted, pressed | Cutoff, U - RER
molybdenum	0.235	kg	market for molybdenum | molybdenum | Cutoff, U - GLO
natural gas, high pressure	0.00743284726980235	m3	market group for natural gas, high pressure | natural gas, high pressure | Cutoff, U - Europe without Switzerland

natural gas, high pressure	4.970132999500146E-5	m3	market for natural gas, high pressure | natural gas, high pressure | Cutoff, U - CH
nitrogen, liquid	0.00359722693195745	kg	market for nitrogen, liquid | nitrogen, liquid | Cutoff, U - RER
oxygen, liquid	0.036	kg	market for oxygen, liquid | oxygen, liquid | Cutoff, U - RER
quicklime, in pieces, loose	0.0591607978309962	kg	market for quicklime, in pieces, loose | quicklime, in pieces, loose | Cutoff, U - CH
refractory, basic, packed	0.0154919333848297	kg	market for refractory, basic, packed | refractory, basic, packed | Cutoff, U - GLO
Water, cooling, unspecified natural origin	0.00654217089351845	m3	
Output			
steel, chromium steel 18/8	1.0	kg	
electric arc furnace dust	2.8657850546607665E-6	kg	market for electric arc furnace dust | electric arc furnace dust | Cutoff, U - CH
electric arc furnace dust	0.019124534214945338	kg	market for electric arc furnace dust | electric arc furnace dust | Cutoff, U - Europe without Switzerland
electric arc furnace secondary metallurgy slag	0.01924	kg	market for electric arc furnace secondary metallurgy slag | electric arc furnace secondary metallurgy slag | Cutoff, U - RER
electric arc furnace slag	0.11089719292129314	kg	market for electric arc furnace slag | electric arc furnace slag | Cutoff, U - Europe without Switzerland
electric arc furnace slag	0.03496880707870686	kg	market for electric arc furnace slag | electric arc furnace slag | Cutoff, U - CH
inert waste, for final disposal	0.00678233	kg	market for inert waste, for final disposal | inert waste, for final disposal | Cutoff, U - CH
Benzene	3.63318042491699E-7	kg	
Cadmium II	1.21655250605964E-8	kg	
Carbon dioxide, fossil	0.0441471958702236	kg	
Carbon monoxide, fossil	4.74341649025257E-4	kg	
Chromium III	1.83303027798234E-7	kg	
Copper ion	7.4899933244296E-8	kg	
Dioxins, measured as 2,3,7,8-tetrachlorodibenzo-p-dioxin	4.89897948556636E-13	kg	
Hexachlorobenzene	1.54919333848297E-9	kg	
Hydrocarbons, aromatic	7.7008E-5	kg	
Hydrochloric acid	5.3103672189407E-6	kg	

Hydrogen fluoride	2.44948974278318E-8	kg	
Lead II	4.62331050222673E-7	kg	
Mercury II	2.0E-8	kg	
Nickel II	7.74596669241483E-8	kg	
Nitrogen oxides	7.73304597167248E-5	kg	
PAH, polycyclic aromatic hydrocarbons	9.34344690143846E-8	kg	
Particulate Matter, < 2.5 um	1.47224318643355E-5	kg	
Particulate Matter, > 10 um	5.19615242270663E-6	kg	
Particulate Matter, > 2.5 um and < 10um	1.47224318643355E-5	kg	
Polychlorinated biphenyls	2.23606797749979E-10	kg	
Sulfur dioxide	3.24037034920393E-5	kg	
Water	0.00292116868798236	m3	
Water	0.00229520396912 9	m3	
Zinc II	2.19089023002066E-6	kg	

Appendix C - Performance benchmarking

Appendix C presents a performance benchmarking summary of existing composite and metallic (steel) bipolar plates. The primary aim is to provide a reference framework for evaluating the potential performance of the novel BPPs developed in this thesis. Table 19 compiles values from 20 literature sources across ten performance categories. Additionally, the 2025 performance targets set by the U.S. Department of Energy (DOE) are included for comparison with the available performance data [44].

Table 19: Performance benchmarking for composite and steel bipolar plates

Properties	**Unit**	**Composite BPP**			**Steel BPP**			**2025 Target**
		Value	**Year**	**Source**	**Value**	**Year**	**Source**	
Electrical Conductivity	S/cm	130.6 331 100	2016 2024 2019	A B C	1400[a]	2021	D	>100
Resistivity	$m\Omega \cdot cm$	8.9 9.6	2023 2024	E F	N/A			< 10
Area-Specific Resistance	$m\Omega \cdot cm^2$	23	2021	G	18 < 10 6 4	2019 2025 2024 2022	H I J K	< 10
In-plane Conductivity	S/cm	177 88.5 182 100	2021 2023 2023 2019	G E L M	N/A			N/A
Through-plane Conductivity	S/cm	38 9.3 50	2021 2023 2019	G E M	N/A			N/A
Cost of Production	$/kW	N/A			5.4 4.8 5.1[b]	2024 2023 2022	J N O,K	2
Weight per Area	kg/m^2	4	2022	K	1.3	2025	I	N/A
Plate weight	kg/kW	0.6[c]	2022	K	0.34[c]	2022	K	0.18
Flexural Strength	MPa	64.9 41.4 45 45 61	2023 2016 2024 2020 2019	E A Q R C	480	2021	O	> 40
Tensile Strength	MPa	33.2 25.2	2023 2016	E A	N/A			N/A

Note: N/A = Not available. a = value for uncoated steel. b = calculated value based on sources [45] & [46]. c = calculated value based on [46].
Sources: A - [47], B - [48], C - [49], D - [50], E - [51], F - [52], G - [53], H - [54], I - [31], J - [55], K - [46], L - [56], M - [57], N - [58], O - [45], Q - [59], R - [60].

DEPARTMENT OF TECHNOLOGY MANAGEMENT AND ECONOMICS
DIVISION OF ENVIRONMENTAL SYSTEMS ANALYSIS
CHALMERS UNIVERSITY OF TECHNOLOGY
Gothenburg, Sweden
www.chalmers.se

CHALMERS
UNIVERSITY OF TECHNOLOGY